COMPOSITE PLASMONIC WAVEGUIDES

Prof. Alina Karabchevsky, www.alinakarabchevsky.com

Integrated Photonics Course 377-2-5599

School of ECE

Ben-Gurion University of the Negev, Israel

OUTLINE

Introduction

Surface plasmon

- Extended surface plasmon
- Localized surface plasmon

Composite-Plasmonic waveguide

- First step $z = 0$
- Second step $z = L$

Invisibility cloaking scheme on composite plasmonic waveguides

Bibliography

INTRODUCTION

- The SPR is a quantum electromagnetic (EM) phenomenon arising from the interaction of light with free electrons at a metal-dielectric interface emerging as a longitudinal EM wave in a two-dimensional gas of charged particles such as free electrons in metals.
- Under certain conditions the energy carried by the photons is transferred to collective excitations of free electrons, called surface plasmons (SPs), at that interface.
- This transfer of energy occurs only at a specific resonance wavelength of light when the momentum of the photon matches that of the plasmon.

INTRODUCTION

- Electron gas in solid, in our case free electrons in metal, can undergo collective motions that call plasma oscillations. It was first presented by Pines and Bohm in 1952. Plasmon is the oscillation of free electrons in plasma or metal.
- Surface plasmon polariton (SPP) are the propagating electromagnetic wave at the interface between a dielectric and a metal.

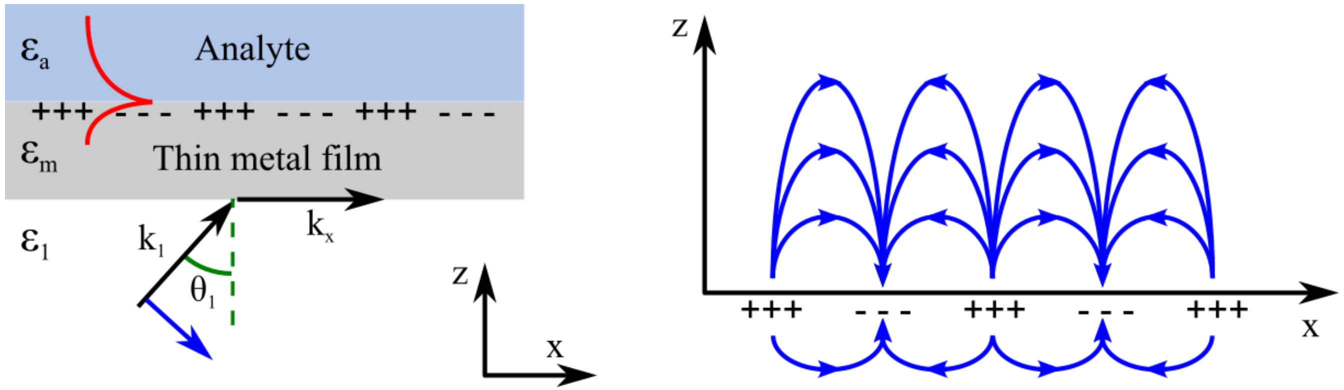

Figure 1: Surface plasmon polariton (SPP) excitation at the interface between thin metal film and analyte and illustration the surface charge density wave.

THE CONDITIONS FOR SP

The conditions for the surface plasmon excitation are:

1. Incident light is TM polarized.
2. The real part of the dielectric constant of the metal and the dielectric are of opposite sign and satisfy: $\Re\{\varepsilon_m\} < -\varepsilon_a$.
3. Wave vector of the incident light is large enough to satisfy the momentum matching $k_x = k_{SP}$.

TM POLARIZED LIGHT

- Propagating SP waves are excited with TM-polarized EM waves when the component of the k-vector along the metal-dielectric interface matches the SP k-vector.
- The condition of TM polarization is needed to generate the charge distribution on the metal-dielectric interface.

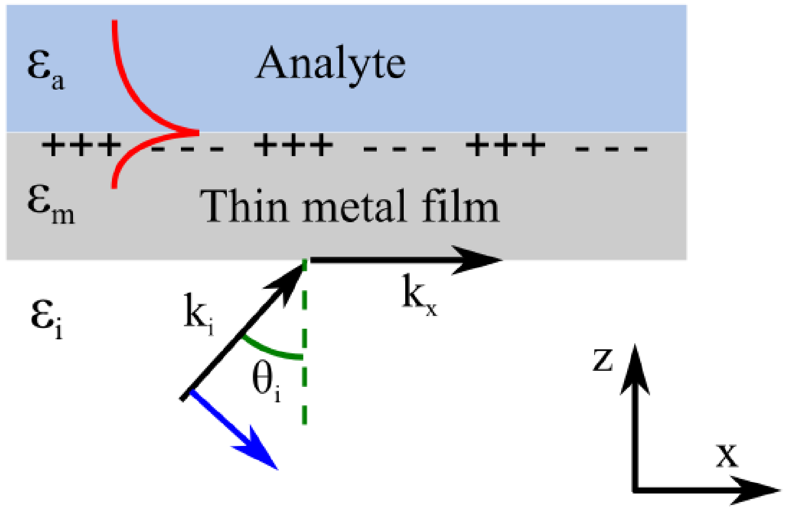

THE MOMENTUM MATCHING

Assuming TM-polarized electro-magnetic wave and applying the continuity relations of the tangential field's components (E_x, H_y):

$$E_i(r,t) = (E_{xi}, 0, E_{zi})e^{j(k_{x,i}x-\omega t)}e^{-jk_{z,i}z} \quad (1)$$

$$H_i(r,t) = \left(0, H_{yi}, 0\right)e^{j(k_{x,i}x-\omega t)}e^{-jk_{z,i}z} \quad (2)$$

where $i = a, m$ is the analyte and metal, respectively (as shown in Fig. 1), and k_z is the z component of the wave vector (k-vector). Since the conversion of the wavevector, we obtain:

$$k_{z,i}{}^2 + k_x{}^2 = \varepsilon_i k^2 \quad (3)$$

where $k = 2\pi/\lambda$ and λ is the vacuum wavelength.

THE MOMENTUM MATCHING

The relationship between the dielectric constants and the normal components of the wavevectors in the two media is given by

$$\frac{k_{z,m}}{\varepsilon_m} + \frac{k_{z,a}}{\varepsilon_a} = 0 \qquad (4)$$

where $\varepsilon = \varepsilon' + j\varepsilon''$ is the relative permittivity. Using Eq. (3) and Eq. (4), the dispersion relation between the wavevector along the propagation direction k_x and the angular frequency ω is defined as:

$$k_x{}^2 = \frac{\varepsilon_m \varepsilon_a}{\varepsilon_m + \varepsilon_a} k^2 = \frac{\varepsilon_m \varepsilon_a}{\varepsilon_m + \varepsilon_a} \left(\frac{\omega}{c}\right)^2 \qquad (5)$$

and the normal component of the wavevector is defined as:

$$k_{z,i}{}^2 = \frac{\varepsilon_i{}^2}{\varepsilon_m + \varepsilon_a} k^2 \qquad (6)$$

THE MOMENTUM MATCHING

The real part of k_x is related to the wavelength of the SPP. Assuming $|\varepsilon''_m| \ll |\varepsilon'_m|$, k'_x is defined as:

$$k'_x \approx \sqrt{\frac{\varepsilon'_m \varepsilon_a}{\varepsilon'_m + \varepsilon_a}} \cdot \frac{\omega}{c} \qquad (7)$$

and the wavelength of the plasmon is given as:

$$\lambda_{\mathrm{SPP}} = \frac{2\pi}{k'_x} \approx \sqrt{\frac{\varepsilon'_m + \varepsilon_a}{\varepsilon'_m \varepsilon_a}} \cdot \lambda \qquad (8)$$

THE MOMENTUM MATCHING

- Since for metal the dielectric constant is negative ($\varepsilon_m < 0$), then $|\varepsilon_m| > \varepsilon_a$.
- From k-vector component in the x direction that is propagating in the metal film ($k_x = k_i n_i \sin\theta_i$) we can calculate the angle for SPR ($\theta_{\text{SPP}} = \theta_i$) where i is the incident angle in the coupling medium.

DECAY LENGTH

Decay length (L_x) is the distance along propagation at which the intensity decays to $1/e$ of the maximum intensity. The damping of the SPP is related to the imaginary part of k''_x. Assuming $|\varepsilon''_m| \ll |\varepsilon'_m|$, k''_x is defined as:

$$k''_x \approx \sqrt{\frac{\varepsilon'_m \varepsilon_a}{\varepsilon'_m + \varepsilon_a}} \cdot \frac{\varepsilon''_m \varepsilon_a}{2\varepsilon'_m(\varepsilon'_m + \varepsilon_a)} \cdot \frac{\omega}{c} \qquad (9)$$

For the intensity, the decay length is equal to $1/(2k''_x)$

$$L_x = \frac{\lambda}{2\pi}\left(\frac{{\varepsilon'_m}^2}{\varepsilon''_m}\right)\left(\frac{\varepsilon_a + \varepsilon'_m}{{\varepsilon_a}^2}\right)^{\frac{3}{2}} \qquad (10)$$

PENETRATION DEPTH

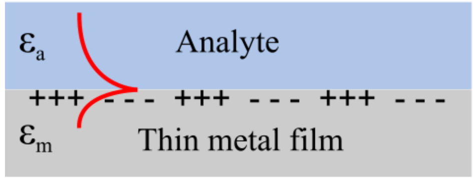

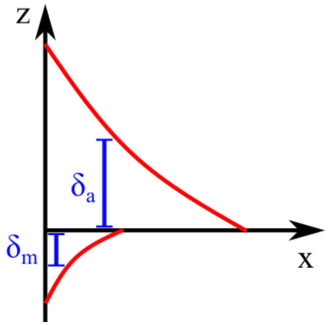

Penetration depth (δ) is the depth from the interface at which the electric field decays to $1/e$ of the maximum intensity. k_{zi} is defined as:

$$k_{z,m} = \frac{\omega}{c}\sqrt{\frac{{\varepsilon'_m}^2}{\varepsilon'_m + \varepsilon'_a}}\left(1 + j\frac{\varepsilon''_m}{\varepsilon'_m}\right) \quad (11)$$

$$k_{z,a} = \frac{\omega}{c}\sqrt{\frac{{\varepsilon_a}^2}{\varepsilon'_m + \varepsilon'_a}}\left[1 - j\frac{\varepsilon''_m}{2(\varepsilon'_m + \varepsilon_a)}\right] \quad (12)$$

PENETRATION DEPTH

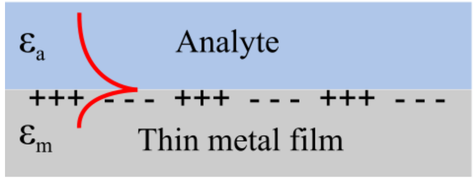

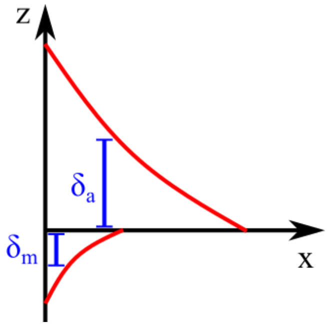

Neglecting the very small imaginary parts, the penetration depth to the analyte is equal to $1/k_{zi}$ and obtained as:

$$\delta_a = \frac{\lambda}{2\pi}\sqrt{\frac{\varepsilon_a + \varepsilon'_m}{{\varepsilon_a}^2}} \qquad (13)$$

while for the penetration depth to the metal film ${\varepsilon_a}^2 \rightarrow {\varepsilon'_m}^2$.

- The penetration depth in the near-infrared (NIR) range is larger by a factor of 8 than that in the visible, although the wavelength ratio is only 2.5. The reason for that is the difference in the real part of the metal dielectric function.

DISPERSION CURVES

- Extended surface plasmon on a flat metal/dielectric interface cannot be excited directly by light since $k_{\mathrm{SP}} > k_i$, prohibiting phase-matching.
- The phase-matching between light and SPPs can be achieved by adding a coupling medium. For large frequencies close to ω_p the damping is negligible due to the product $\omega\tau \gg 1$ and then $\varepsilon(\omega)$ is predominantly real.
- Here, the coupling medium allows for the phase matching. The graph shows the dispersion curves for incident light into the metal from vacuum and SF11 at incidence angle of 50 degrees.

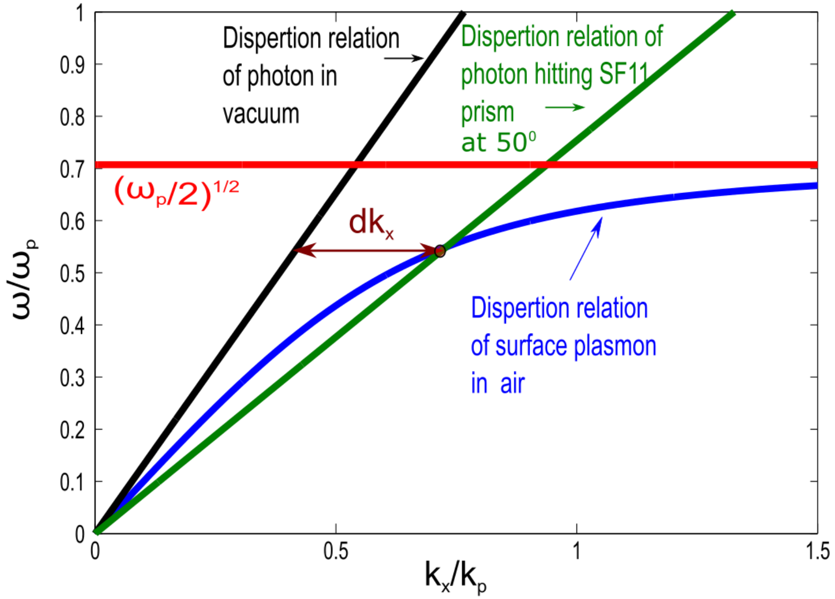

Figure 2: Dispersion curves of prism coupling.

CONFIGURATIONS FOR EXTENDED SPR EXCITATION

Plasmons can't be excited directly by electromagnetic radiation due to the needed momentum conservation. The phase velocity of the plasmon is smaller than the phase velocity of the light in vacuum. Therefore, the momentum of the photons is smaller than the momentum of the plasmon.

In order to fulfill the matching condition, the electromagnetic radiation needs to couple to excite the plasmon by evanescent field. There are three configurations for excitation of SPR:

- Grating configuration.
- Otto configuration.
- Kretschmann-Raether configuration.

GRATING CONFIGURATION

Another option is to excite plasmon by using a metal grating.

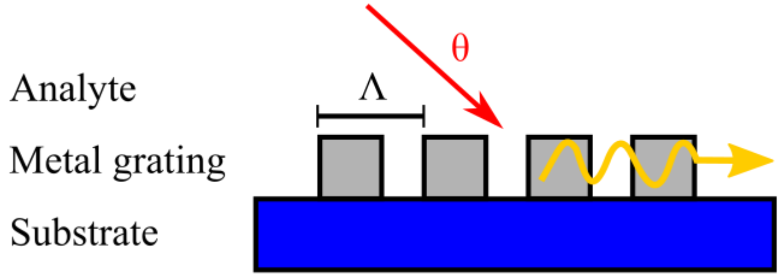

Note: The grating can be dielectric on metal substrate or metallic on dielectric substrate.

GRATING CONFIGURATION

In order to excite plasmon in the grating, the matching between the grating constant, the incident light and the plasmonic wave is needed:

$$\frac{2\pi}{\lambda} n_a \sin\theta \pm \frac{2\lambda}{\Lambda} m = \frac{2\pi}{\lambda}\sqrt{\frac{\varepsilon_m \varepsilon_{a,s}}{\varepsilon_m + \varepsilon_{a,s}}} \tag{14}$$

where Λ is the grating constant and a, s corresponds to the medium where the plasmonic wave will propagate (analyte or substrate).

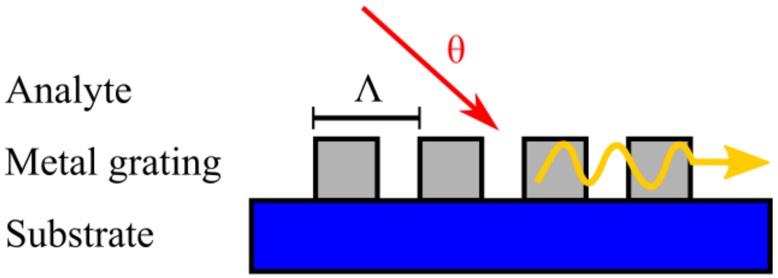

Figure 3: Illustration of grating configuration for SPR excitation.

GRATING EXPERIMENT

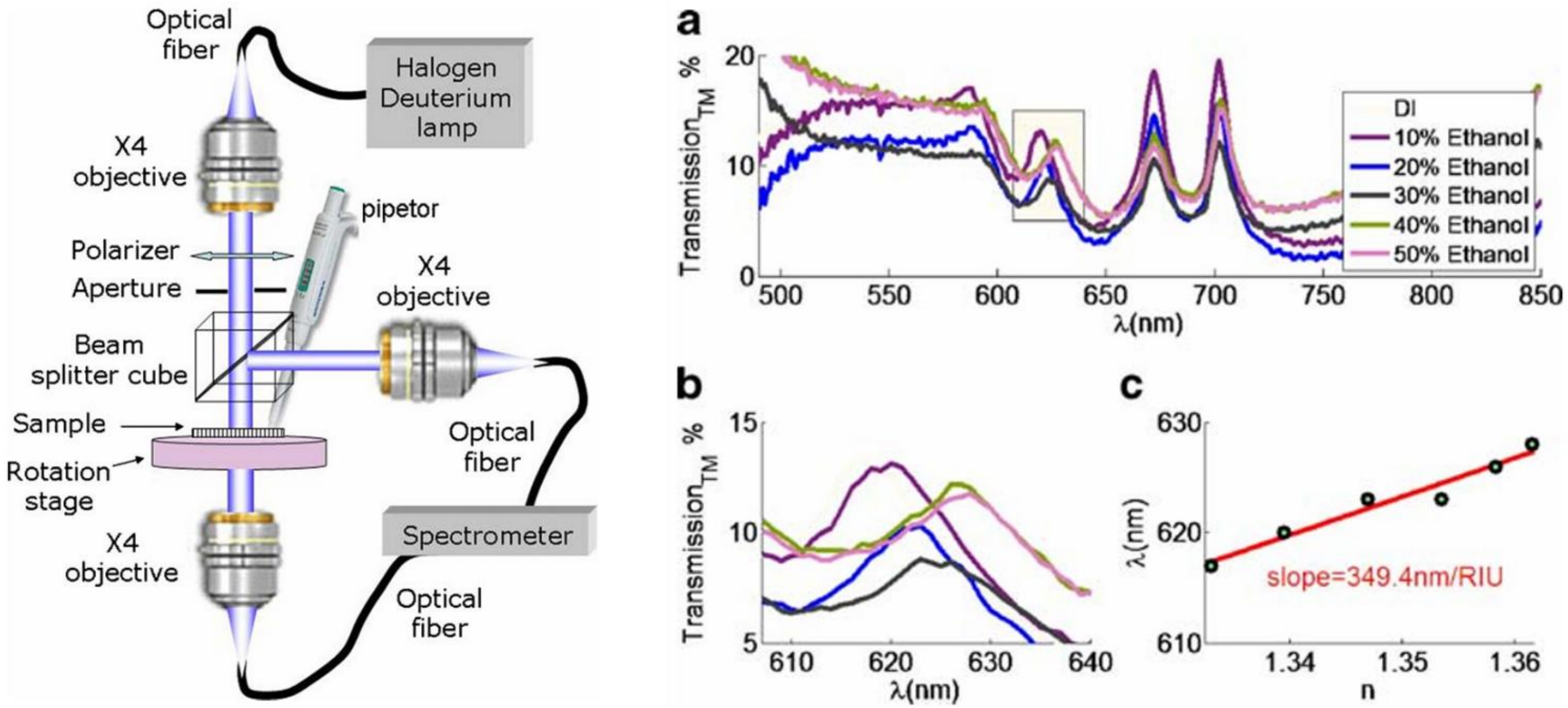

Figure 4: (left) Schematic of the experimental setup of grating configuration for SPR excitation and (right) experimental results [1].

OTTO CONFIGURATION

In Otto configuration there is an air between the prism and the metal layer and the plasmon propagates on the surface of the metal film.

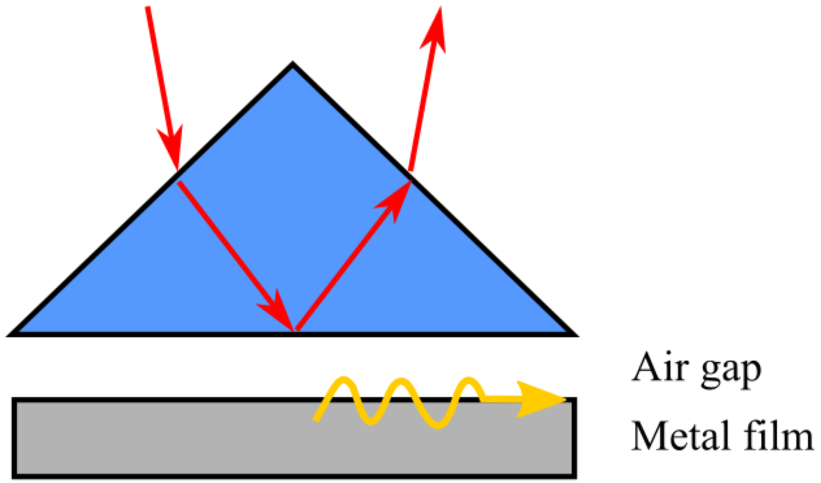

Figure 5: Illustration of Otto configuration for SPR excitation.

KRETSCHMANN-RAETHER CONFIGURATION

In Kretschmann-Raether configuration, the metal layer is deposited on the prism and the plasmon propagates on the metal-air boundary.

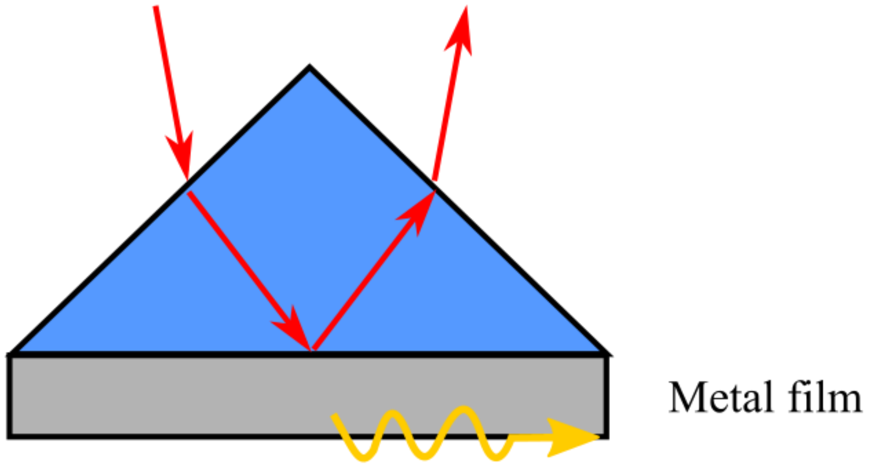

Figure 6: Illustration of basic Kretschmann-Raether configuration for SPR excitation.

COMPERING BETWEEN PRISM COUPLING METHODS

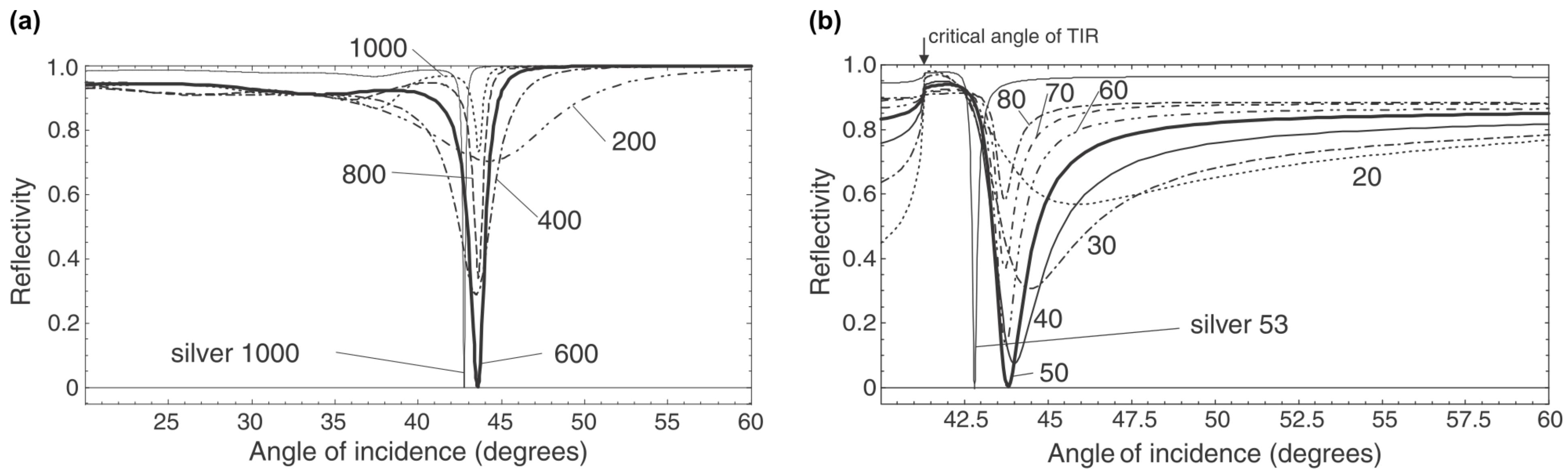

Figure 7: Excitation of surface plasmons for different thicknesses of a gold film on glass (in nanometers) at wavelength of 632.8 nm in (a) Otto configuration and (b) Kretschmann-Raether configuration [2].

SURFACE PLASMON SENSORS

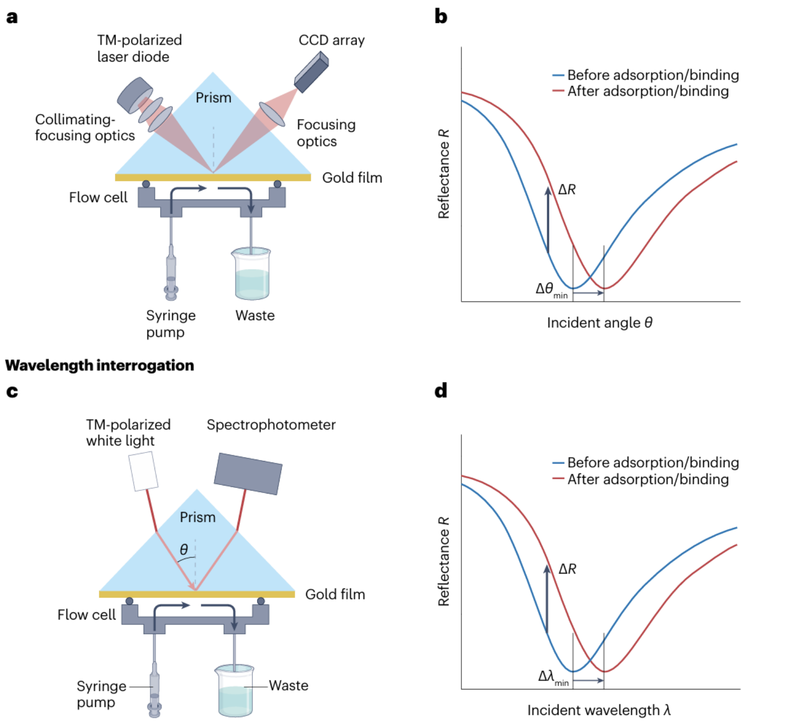

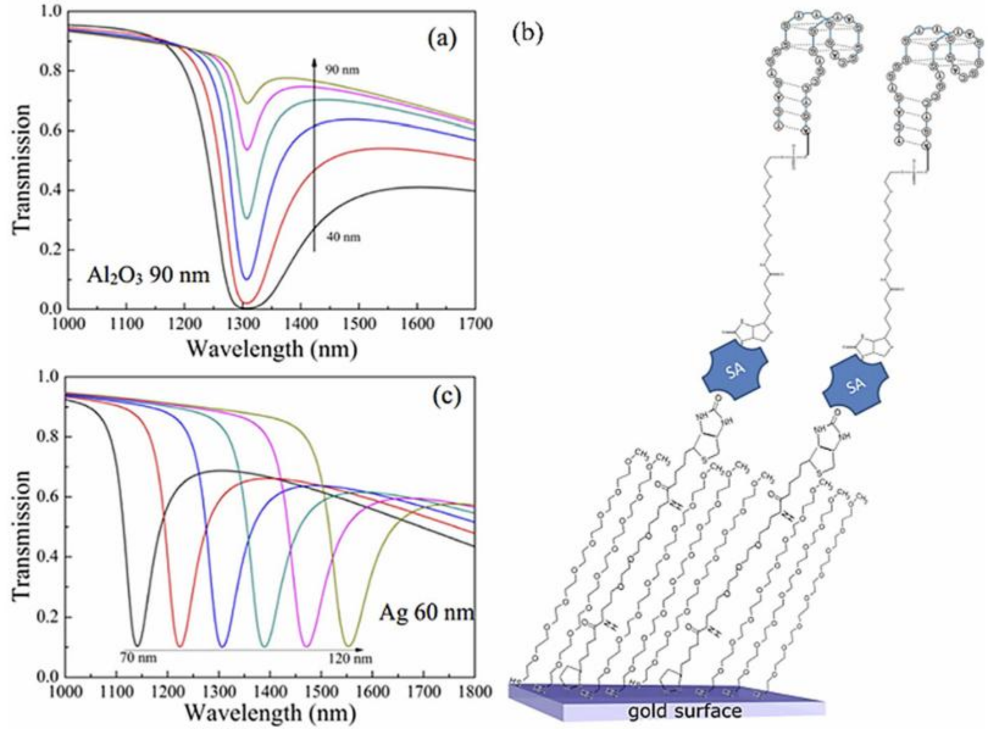

Figure 8: (left) Prism-based optical set-ups and SPR detection modes [3]. (a) Transmission spectra of the SPR sensor with different Al2O3 thicknesses, (b) functionalization process, and (c) SPR transmission spectra for different concentrations of thrombin (1-80 nM).(right) [4].

LOCALIZED SURFACE PLASMON (LSP)

When the metal layer is made of subwavelength ($d \ll \lambda$) structural units (such as nanoparticles, containing nanoholes, etc.), the plasmon becomes localized and non-propagating. It can't propagate more than the size of the structural unit.

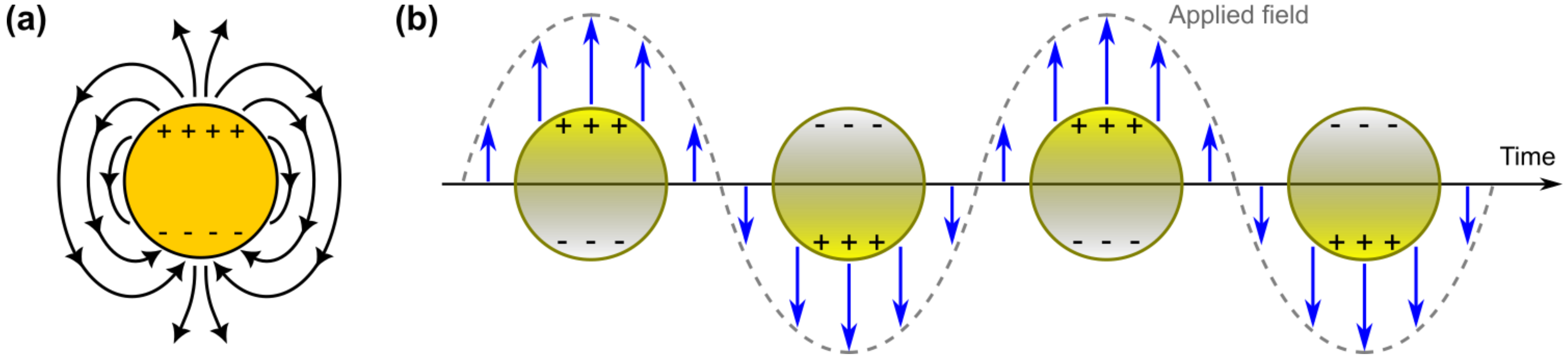

Figure 9: (a) Illustration of the surface charge density of an LSP. (b) Oscillations of free electrons at the surface of a nanosphere due to applied electric field with arbitrary polarization.

LOCALIZED SURFACE PLASMON (LSP)

The LSP can be described by the polarizability α of the particle

$$\alpha = \frac{p}{E} \tag{15}$$

where p is the electric dipole moment and E is the applied electric field.

For example, For spherical particle with radius smaller than the wavelength of the incident radiation, we obtain:

$$C_{\text{scat}} = \frac{8\pi}{3} k^4 r^6 \left| \frac{\varepsilon_{\text{sph}} - \varepsilon_s}{\varepsilon_{\text{sph}} + 2\varepsilon_s} \right| = \frac{k^4}{6\pi} \left| \alpha_{\text{sph}} \right|^2 \quad \Rightarrow \quad C_{\text{scat}} \propto \frac{r^6}{\lambda^4} \tag{16}$$

$$C_{\text{abs}} = 4\pi k r^3 \Im \left\{ \frac{\varepsilon_{\text{sph}} - \varepsilon_s}{\varepsilon_{\text{sph}} + 2\varepsilon_s} \right\} = k \Im \{ \alpha_{\text{sph}} \} \quad \Rightarrow \quad C_{\text{abs}} \propto \frac{r^3}{\lambda} \tag{17}$$

LOCALIZED SURFACE PLASMON (LSP)

α_{sph} is the polarizability of a spherical particle with radius r:

$$\alpha_{\text{sph}} = 4\pi\varepsilon_0 r^3 \frac{\varepsilon_{\text{sph}} - \varepsilon_s}{\varepsilon_{\text{sph}} + 2\varepsilon_s} \tag{18}$$

where ε_{sph} the dielectric function of the sphere, ε_s the dielectric function of the surrounding medium and k is the wavevector. For metal sphere, the dielectric function of the sphere can be approximated by Drude model as:

$$\varepsilon_{\text{sph}} = \varepsilon_m = 1 - \frac{{\omega_p}^2}{\omega(\omega + j\gamma)} \tag{19}$$

where γ is the damping of the electrons and ω_p is the plasma frequency.

LOCALIZED SURFACE PLASMON (LSP)

Ancient 4th century Lycurgus cup shows the effect of plasmons in nanoparticles. When illuminated with white light from the behind shows a red color, while when illuminated from the front appears green. The effect is due to the interplay between scattering and absorption.

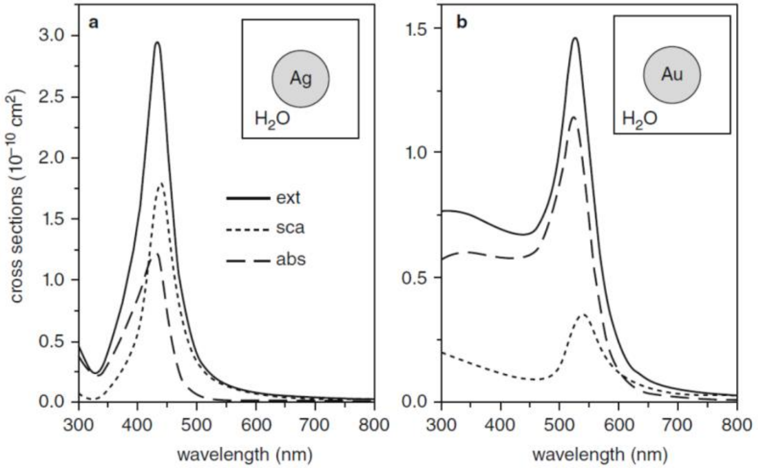

Figure 10: (Left) Ancient Roman Lycurgus cup exhibited at the British Museum. (Right) Cross-sections of extinction, scattering, and absorption [5].

APPLICATIONS FOR LSP

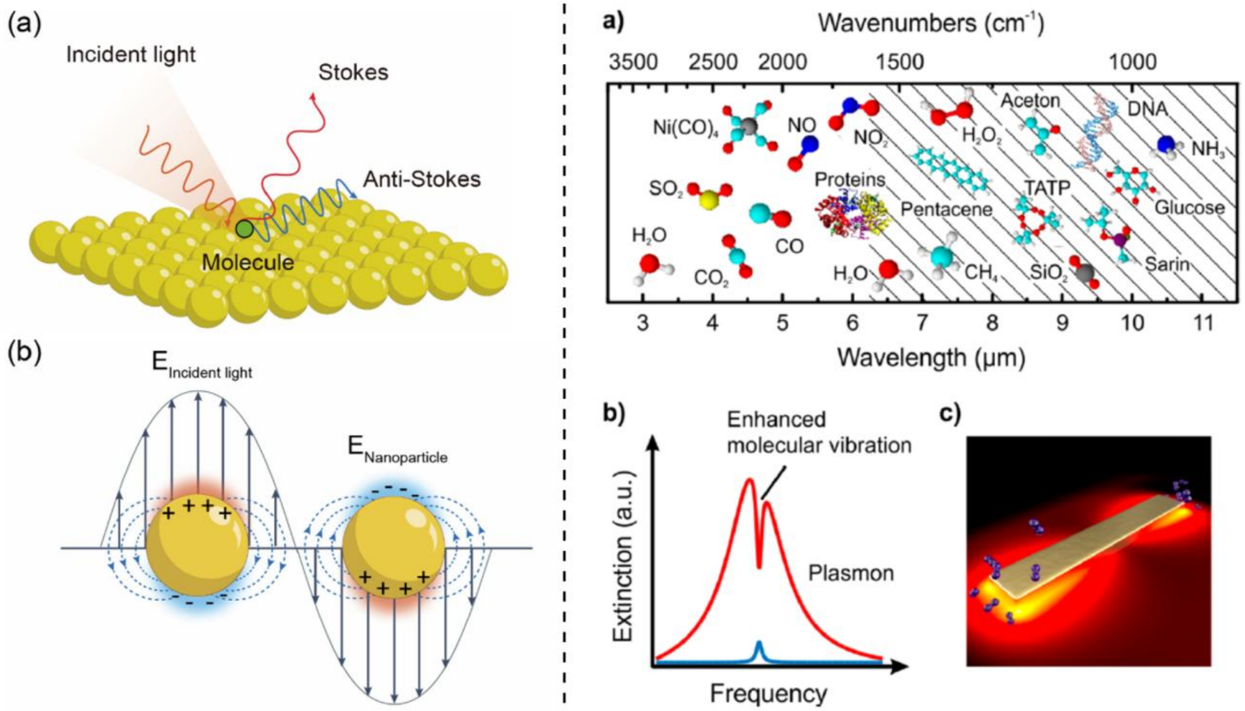

Figure 11: Field-enhanced vibrational spectroscopy: (left) surface-enhanced raman spectroscopy (SERS) [6] and (right) surface-enhanced infrared spectroscopy (SEIRA) [7].

HYBRID PLASMONIC DEVICES

- Hybrid plasmonic devices incorporating dielectric and metallic waveguiding structures offer great potential for ultra-compact high-performance devices from polarizers and sensors, through surface-enhanced Raman spectrometers, to telecommunications filters and all-optical switches. In particular there is growing interest in such plasmonic technologies for biochemical analysis in clinical point-of-care applications.
- Surface plasmon-polaritons (SPP) are supported by several different optical waveguide configurations. Thin metal films sandwiched between two semi-infinite dielectric media are known to support bound and leaky SPP modes with symmetric and anti-symmetric transverse-magnetic field distributions across the film thickness.

HYBRID PLASMONIC DEVICES

Hybrid plasmonic devices can be used for a variety of applications such as polarizers, filters, modulators and switches.

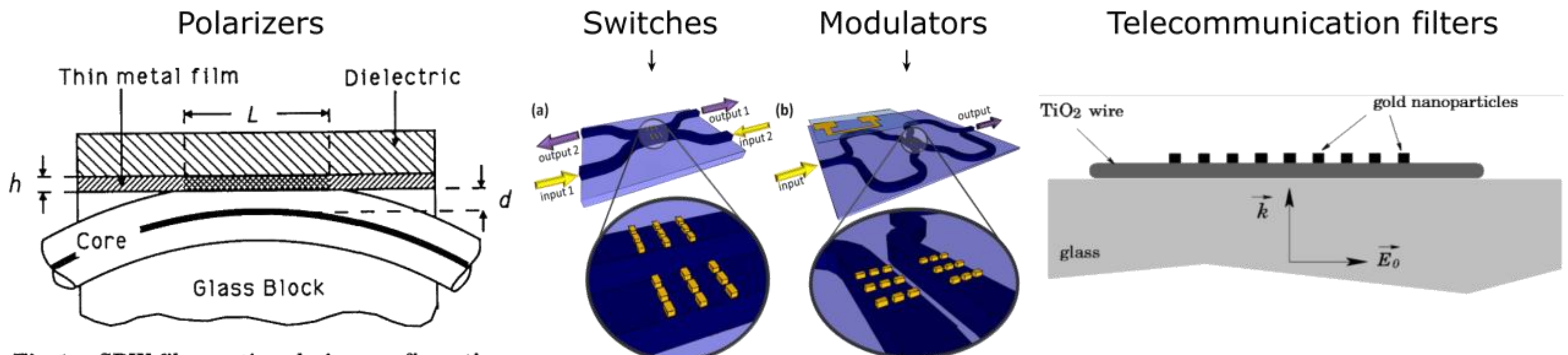

Fig. 1. SPW fiber-optic polarizer configuration.

Figure 12: Hybrid plasmonic devices incorporating dielectric and metallic guided wave structures.

THE STRUCTURE

- Here we consider the 3D composite plasmonic waveguide which is modeled throughout at a wavelength of 633 nm [8].
- It consists of a dielectric ridge waveguide with core having index of $n_1 = 1.478$, width of 4 μm and height of 2 μm, covered by a 50 nm thick gold stripe with complex index of $0.197 - 3.466j$ over a finite length L, the refractive index of the substrate $n_2 = 1.471$. The superstrate index was chosen to vary from 1.3 to 1.44.

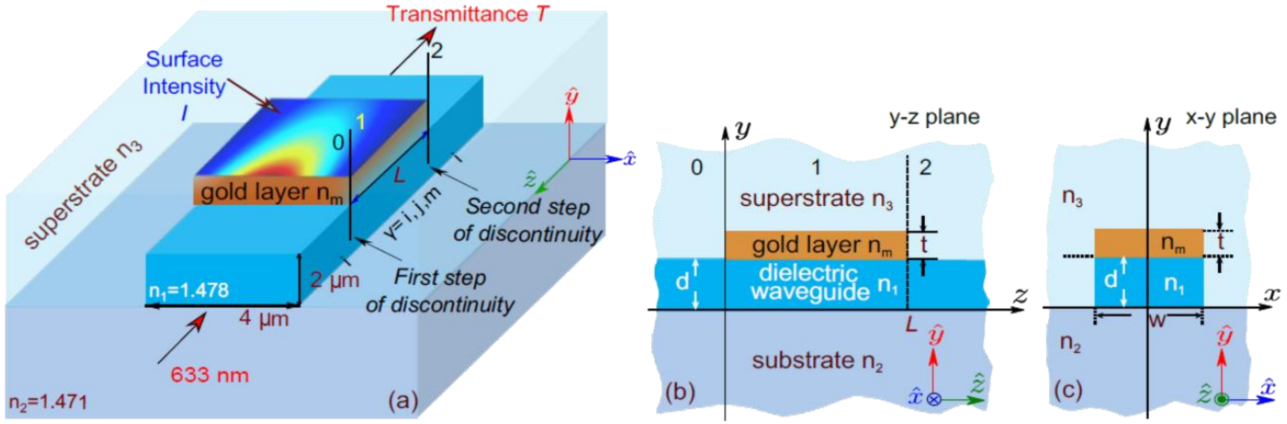

Alina Karabchevsky, James S Wilkinson, and Michalis N Zervas. Transmittance and surface intensity in 3d composite plasmonic waveguides. Optics express, 23(11):14407-14423, 2015.

OPTICAL THEOREM AND COMPLEX INDEX OF REFRACTION

The index of refraction is linearly related to the forward scattering amplitude

$$n = 1 + 2\pi N k^{-2} S(0)$$

Forward scattering amplitude $S(0)$ of a medium having N particles per unit volume and reduced wavenumber of light is $k_d = \frac{\omega}{c} = 2\pi(n + j\kappa)/\lambda_0$.

Using $\sigma_{\text{tot}} = \sigma_{\text{ext}} = 4\pi N k^{-1} \mathcal{L}S(0)$ we obtain relation of dispersion of light by Kramers-Kronig (KK) considering causal propagation of radiation in a medium. The dispersion relation is gives as

$$\mathcal{R}S(0, \omega) \ = \frac{1}{2\pi^2 C} \mathcal{P} \int_0^{\infty} \frac{\omega' \sigma_{\text{tot}}(\omega')}{\omega'^2 - \omega^2} d\omega'$$

This is the Hilbert transform relation between the real and the imaginary parts of the refractive index as a function of frequency.

KRAMERS-KRONIG RELATIONS

Kramers-Kronig relation can be used to calculate the complex refractive index of a material.

$$n(\omega) - 1 = \frac{2}{\pi}\mathcal{P}\int_0^\infty \frac{\omega'\kappa(\omega')}{\omega'^2 - \omega^2}d\omega' \tag{20}$$

$$\kappa(\omega) = -\frac{2\omega}{\pi}\mathcal{P}\int_0^\infty \frac{n(\omega') - 1}{\omega'^2 - \omega^2}d\omega' \tag{21}$$

where $\mathcal{P}$ is the Cauchy principal value and the complex refractive index is $\tilde{n} = n + j\kappa$.

DISPERSION OF A MEDIUM

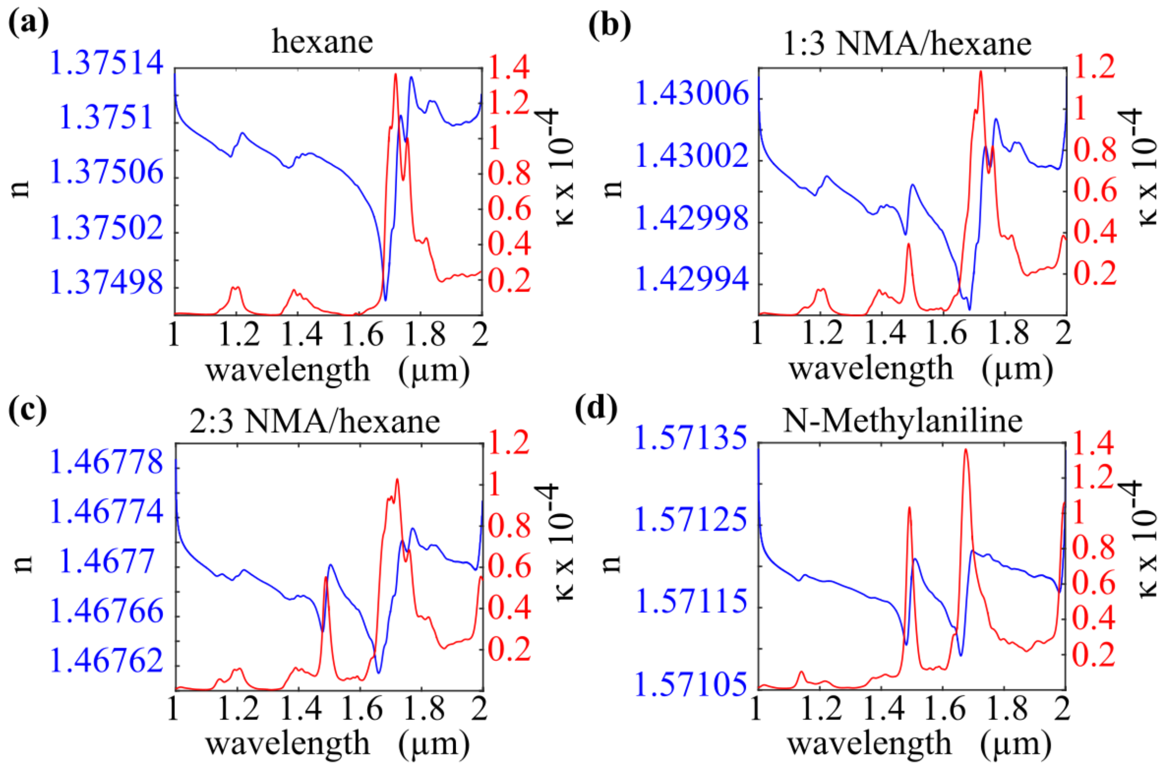

Figure 13: Dispersions calculated by using the KK relations.

H.W.

1. Derive the KK dispersion relation between forward scattering amplitude and the total cross-section.
2. Derive the KK dispersion relation between refractive index and extinction coefficient.
3. Why imaginary part of complex optical index is named extinction coefficient?
4. Why the real part of complex optical index has geometrical meaning?
5. Explain the physical meaning of the causality in Eqs. (20)-(21).

MODAL COUPLING ACROSS DISCONTINUITIES IN WAVEGUIDES

The discontinuity in the waveguide will produce a reflected guided mode E_r and forward E_{fr} and backward E_{br} traveling radiation modes as well as the transmitted guided mode E_t. The continuity of the electromagnetic fields across the discontinuity will then give, for TE modes

$$E_i + E_r + E_{br} = E_t + E_{fr} \qquad (22)$$

where i, r, t are incident, reflected and transmitted guided modes, respectively. fr and br are forward $S(0)$ and backward $S(\pi)$ scattered radiation modes. Only E_i represents a single mode.

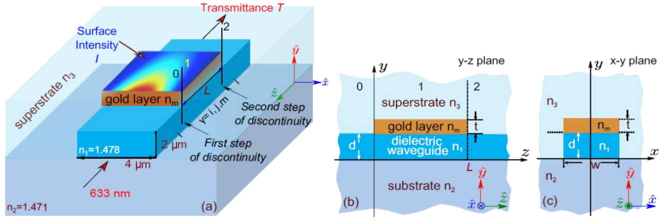

FIELD DISTRIBUTIONS - $z = 0\ \mu m$

The general complex field distributions at the boundary between input waveguide and waveguide with gold overlayer, while ignoring reflected and radiated modes, are:

$$E_{xi0} = \sum_{\gamma=i,j,m} E_{x\gamma 1} \qquad E_{yi0} = \sum_{\gamma=i,j,m} E_{y\gamma 1} \qquad (23,24)$$

$$H_{xi0} = \sum_{\gamma=i,j,m} H_{x\gamma 1} \qquad H_{yi0} = \sum_{\gamma=i,j,m} H_{y\gamma 1} \qquad (24,25)$$

$\boldsymbol{E} = E_x\hat{x} + E_y\hat{y} + E_z\hat{z}$ and $\boldsymbol{H} = H_x\hat{x} + H_y\hat{y} + H_z\hat{z}$ where $\hat{x}$, $\hat{y}$ and $\hat{z}$ are unit vectors in the x, y and z directions, respectively.

BONUS

The task:

Derive transmittance and surface intensity while considering reflected and radiated modes.

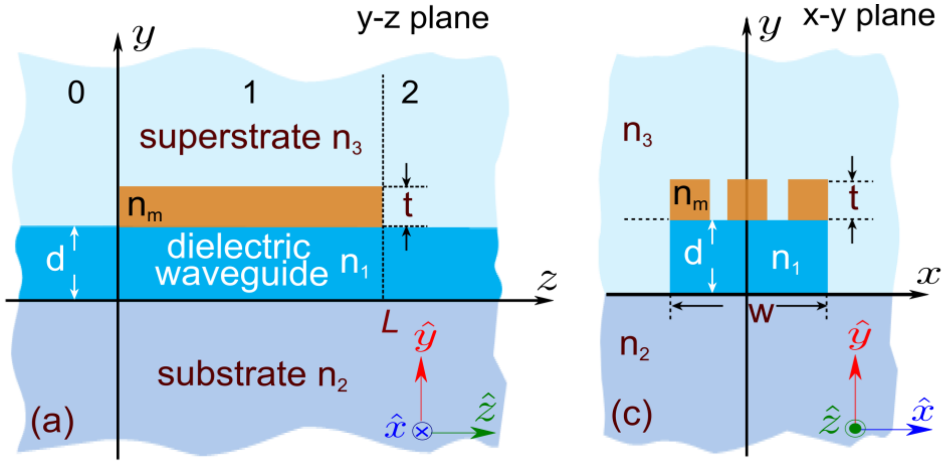

Figure 14: Plasmonic grating overlayer.

CROSS-SECTIONS OF ε_y

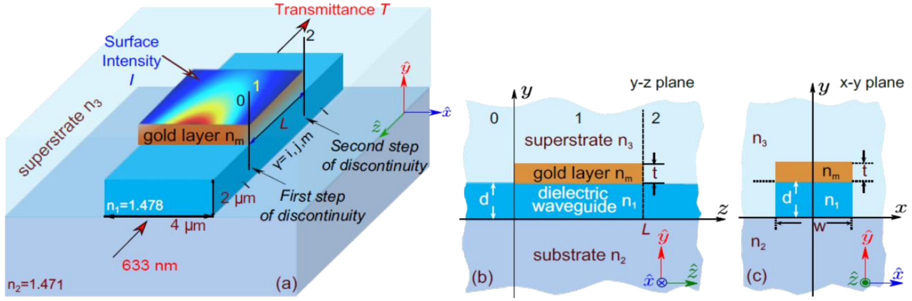

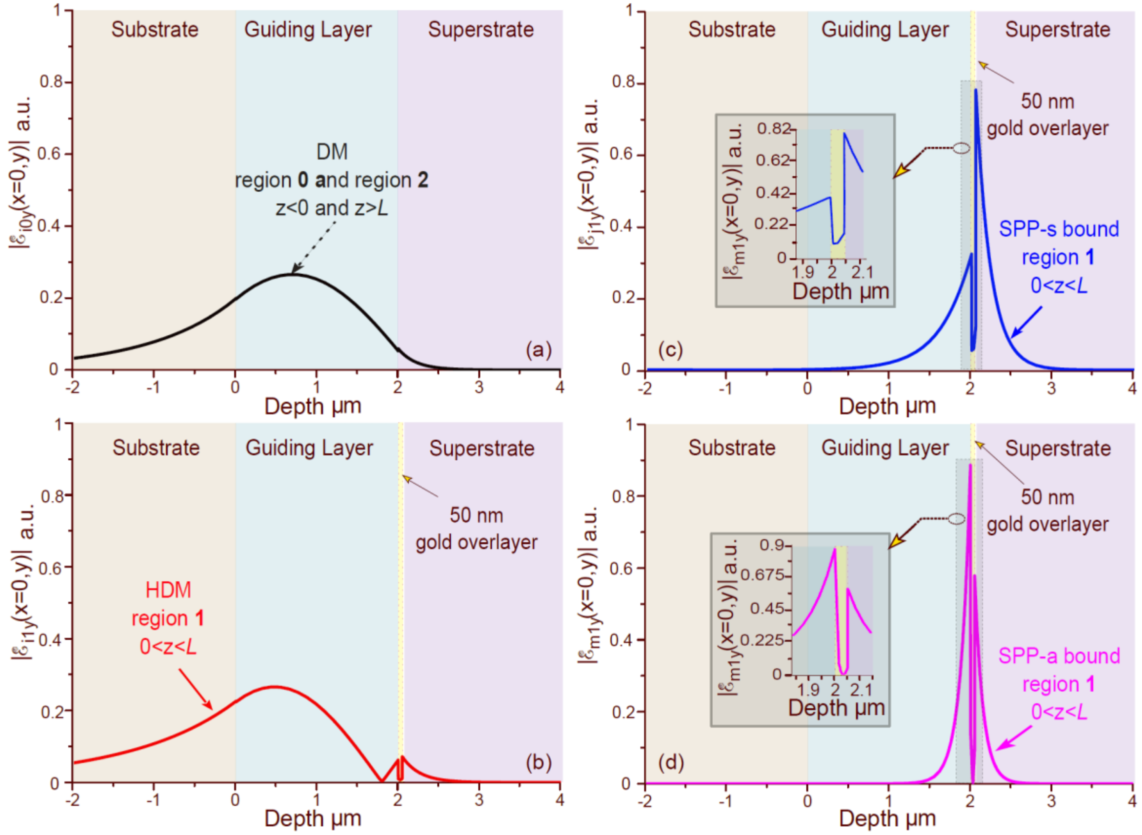

Figure 15: Cross-sections of the y component of the electric field magnitude for the structure shown in Fig. 10 with a superstrate index of 1.4 for different regions [8].

Alina Karabchevsky, James S Wilkinson, and Michalis N Zervas. Transmittance and surface intensity in 3d composite plasmonic waveguides. Optics express, 23(11):14407-14423, 2015.

MODE-MATCHING

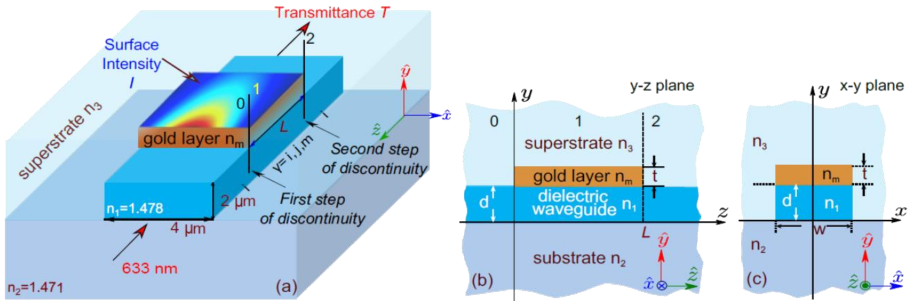

$$E_{\xi i0} = \sum_{\gamma=i,j,m} E_{\xi\gamma 1} \qquad H_{\xi i0} = \sum_{\gamma=i,j,m} H_{\xi\gamma 1} \qquad (27,28)$$

where $\xi = x, y$. An expression for the expansion coefficient between input mode $i0$ in region 0 and mode $j1$ in region 1 is derived using the complex orthogonality principle:

$$\frac{\iint_{-\infty}^{\infty} \left[\left(\mathbf{E}_{i0} \times \mathbf{H}_{\gamma 1}\right)_z + \left(\mathbf{E}_{\gamma 1} \times \mathbf{H}_{i0}\right)_z\right] dxdy =}{\iint_{-\infty}^{\infty} \left[\left(\mathbf{E}_{\gamma 1} \times \mathbf{H}_{\gamma 1}\right)_z + \left(\mathbf{E}_{\gamma 1} \times \mathbf{H}_{\gamma 1}\right)_z\right] dxdy} \qquad (29)$$

where $\gamma 1 = i1, j1, m1$.

EXPRESSION OF THE EXPANSION COEFFICIENTS

To derive the expression of the expansion coefficient between input mode i at the 0 side of the first step and mode j at the gold coated side of the first step 1. Multiplying Eq. (23) by H_{yj1} and Eq. (24) by H_{xj1} and subtracting between them leads to:

$$E_{xi0}H_{yj1} - E_{yi0}H_{xj1} = E_{xj1}H_{yj1} - E_{yj1}H_{xj1} \qquad (30)$$

Multiplying Eq. (10) by E_{yj1} and Eq. (11) by E_{xj1} and subtracting between them leads to:

$$-\left(E_{yj1}H_{xi0} - E_{xj1}H_{yi0}\right) = -(E_{yz1}H_{xj1} - E_{xj1}H_{yj1}) \qquad (31)$$

Which is simply:

$$E_{xj1}H_{yi0} - E_{yj1}H_{xi0} = E_{xj1}H_{yj1} - E_{yj1}H_{xj1} \qquad (32)$$

In Eq. (30)-(32), complex orthogonality principle has been considered. Therefore, $\gamma \neq j$ and $I_{\gamma,j} = 0$ at steps 1 and 2.

POWER CARRIED BY MODE j ON SIDE 1 OF DISCONTINUITY

By adding Eq. (30) and Eq. (32) and integrating over a whole range we obtain power carried in a mode j on the side 1 of the first abrupt step:

$$\begin{aligned}&\iint_{-\infty}^{\infty}\left[\left(\mathbf{E}_{i0}\times\mathbf{H}_{j1}\right)_z+\left(\mathbf{E}_{j1}\times\mathbf{H}_{i0}\right)_z\right]dxdy\\&=\iint_{-\infty}^{\infty}\left[2\left(\mathbf{E}_{j1}\times\mathbf{H}_{j1}\right)_z\right]dxdy\end{aligned}\tag{33}$$

General complex electric and magnetic field distribution components:

$$\mathbf{E}_\delta(x,y,z)=a_\delta\overline{\mathcal{E}}_\delta(x,y)\exp(-j\beta_\delta z)\tag{34}$$

$$\mathbf{H}_\delta(x,y,z)=a_\delta\overline{\mathcal{H}}_\delta(x,y)\exp(-j\beta_\delta z)\tag{35}$$

where $z=0$ at the first step, β_δ is a propagation constant of mode δ and $\overline{\mathcal{E}}_\delta(x,y)$ and $\overline{\mathcal{H}}_\delta(x,y)$ are extracted complex field components.

RELATION BETWEEN EIGENMODES AT AN ABRUPT STEP

By substituting Eq. (34) and Eq. (35) into Eq. (33) we obtain:

$$a_{i0}\cancel{a_{\gamma 1}} \iint_{-\infty}^{\infty} \left[\left(\bar{\mathcal{E}}_{i0} \times \bar{\mathcal{H}}_{\gamma 1} \right)_z + \left(\bar{\mathcal{E}}_{\gamma 1} \times \bar{\mathcal{H}}_{i0} \right)_z \right] dxdy =$$
$$= \left(a_{\gamma 1} \right)^{\cancel{2}} \iint_{-\infty}^{\infty} 2 \left[\left(\bar{\mathcal{E}}_{\gamma 1} \times \bar{\mathcal{H}}_{\gamma 1} \right)_z \right] dxdy = \quad (36)$$

To obtain a relation between eigenmodes at an abrupt step:

$$a_{i0}\left(I_{i0,\gamma 1} + I_{\gamma 1,i0} \right) = a_{\gamma 1} 2 I_{\gamma 1,\gamma 1}$$
$$a_{\gamma 1} = a_{i0} \frac{I_{i0,\gamma 1} + I_{\gamma 1,i0}}{2 I_{\gamma 1,\gamma 1}} \quad (37)$$

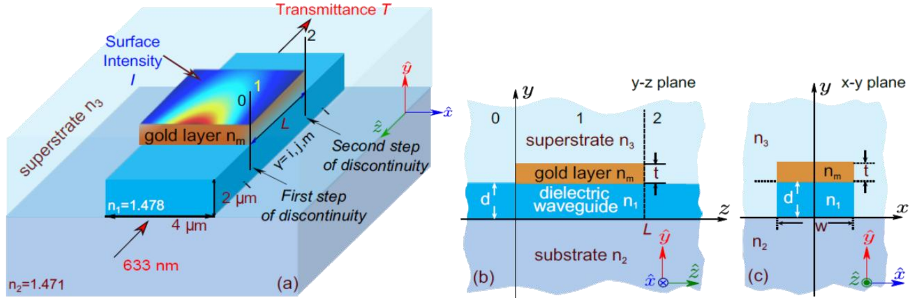

EIGENMODES

where

$$I_{i,\gamma} = \iint_{-\infty}^{\infty} \left[\left(\overline{\mathcal{E}}_i \times \overline{\mathcal{H}}_\gamma \right)_z \right] dxdy = \iint_{-\infty}^{\infty} \left(\mathcal{E}_{xi}\mathcal{H}_{y\gamma} - \mathcal{E}_{yi}\mathcal{H}_{x\gamma} \right) dxdy$$

Let define complex A_δ

$$A_\delta = |A_\delta| \exp(-j\phi_\delta) \tag{38}$$

A_δ is related to the power carried by a mode as:

$$P_\delta = |A_\delta|^2 \tag{39}$$

The aim: each mode carrying power of unity: $P_\delta = 1$

NORMALIZATION OF EIGENMODES

$$a_\delta = N_\delta A_\delta = \frac{E_\delta(x,y,z)}{\mathcal{E}_\delta(x,y)\exp(-j\beta_\delta z)} \tag{40}$$

The normalization factor having unity power:

$$N_\delta = \left(\frac{2}{\Re\left\{\iint_{-\infty}^{\infty}\left(\overline{\mathcal{E}}_i \times \overline{\mathcal{H}}_\gamma^*\right)_z dxdy\right\}}\right)^{1/2} \tag{41}$$

where

$$\overline{\mathcal{E}} = \mathcal{E}_x\hat{x} + \mathcal{E}_y\hat{y} + \mathcal{E}_z\hat{z}$$
$$\overline{\mathcal{H}} = \mathcal{H}_x\hat{x} + \mathcal{H}_y\hat{y} + \mathcal{H}_z\hat{z}$$

NORMALIZATION

We express normalization factor N_δ as:

$$N_\delta = \sqrt{\frac{2}{\Re\{I_{\delta,\delta}\}}} \tag{42}$$

Which is:

$$A_{\gamma 1} N_{\gamma 1} = \frac{A_{\gamma 0} N_{\gamma 0} \left(I_{i0,\gamma 1} + I_{\gamma 1, i0} \right)}{2 I_{\gamma 1,\gamma 1}} \tag{43}$$

Let define expansion coefficient $c_{i0,\gamma 1}$:

$$c_{i0,\gamma 1} = \frac{a_{\gamma 1}}{a_{i0}} = \frac{N_{i0}}{N_{j1}} \cdot \frac{I_{i0,j1} + I_{j1,i0}}{2 I_{j1,j1}} \tag{44}$$

which expands mode i at 0 side into mode j at side 1 of 1^{st} abrupt step.

EXPANSION COEFFICIENT

For $z = 0$:

$$a_{i0}\mathcal{H}_{\xi i0} = \sum_{\gamma=i,j,m} a_{\gamma 1}\mathcal{H}_{\xi\gamma 1} \qquad a_{i0}\mathcal{E}_{\xi i0} = \sum_{\gamma=i,j,m} a_{\gamma 1}\mathcal{E}_{\xi\gamma 1}$$

The power in any region is defined as:

$$P = \frac{1}{2}\Re\left\{\iint_{-\infty}^{\infty}(\mathcal{E}\times\mathcal{H}^{*})_z dxdy\right\} \qquad (45)$$

An expansion coefficient $c_{i0,\gamma 1}$ expanding mode $i1$ from region 0 into mode $\gamma 1$ in region 1 over the first abrupt step is:

$$c_{i0,\gamma 1} = \frac{a_{\gamma 1}}{a_{i0}} = \frac{N_{i0}}{N_{\gamma 1}} \cdot \frac{I_{i0,\gamma 1} + I_{\gamma 1,i0}}{2I_{\gamma 1,\gamma 1}} \qquad (46)$$

EXPANSION COEFFICIENT

At $z = L$, the expansion coefficients are derived in a similar manner to that detailed above resulting in:

$$c_{i1,\gamma 2} = \frac{I_{\gamma 1,j2} + I_{i2,\gamma 1}}{2I_{i2,i2}} \exp[-j(\beta_{\gamma 2} - \beta_{i1})L] \quad (47)$$

Since $a_{\gamma 1} = c_{i0,\gamma 1} a_{i0}$

$$a_{i2} = c_{i0,\gamma 1} a_{i0} c_{\gamma 1,i2} \quad (48)$$

or

$$A_{i2} N_{i2} = c_{i0,\gamma 1} A_{i0} N_{i0} c_{\gamma 1,i2} \quad (49)$$

BONUS

The task:

1. Derive expansion coefficients considering reflection and radiation modes when $z = L$.

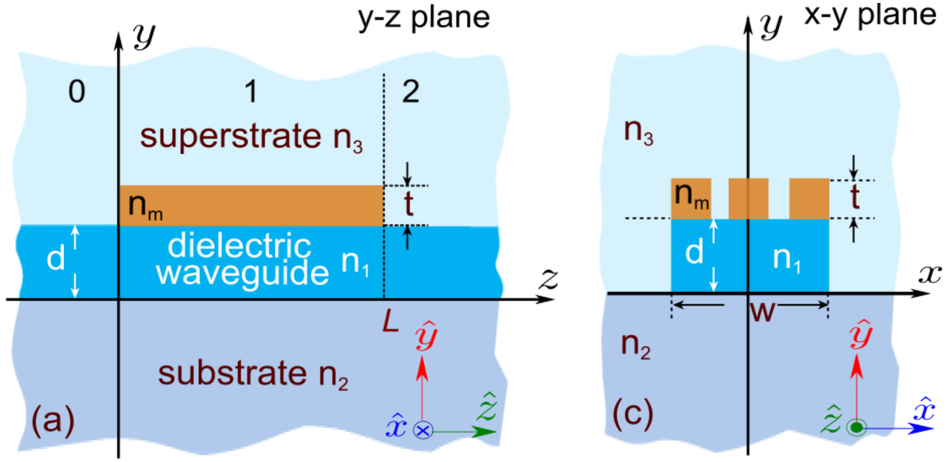

Figure 16: Plasmonic grating overlayer [8].

SURFACE INTENSITY

where $\mathcal{E}_1$ and $\mathcal{H}_1$

$$\mathcal{E}_1 = \sum_{\gamma=i,j,m} c_{i0,\gamma 1}\mathcal{E}_{\gamma 1} \qquad \mathcal{H}_1 = \sum_{\gamma=i,j,m} c_{i0,\gamma 1}\mathcal{H}_{\gamma 1}$$

$P_1/P_0 < 1$ and surface intensity of, for example, the y component of an electric field (normalized to the complex input field amplitude a_{i0}) is:

$$\text{Intensity} = |E(x, y_s, z)|^2 = \left| \sum_{\gamma=i,j,m} c_{i0,\gamma 1}\mathcal{E}_{y\gamma 1}(x, y_s, z) \right|^2 \qquad (50)$$

where $y_s = d + t$

CALCULATED SURFACE INTENSITY

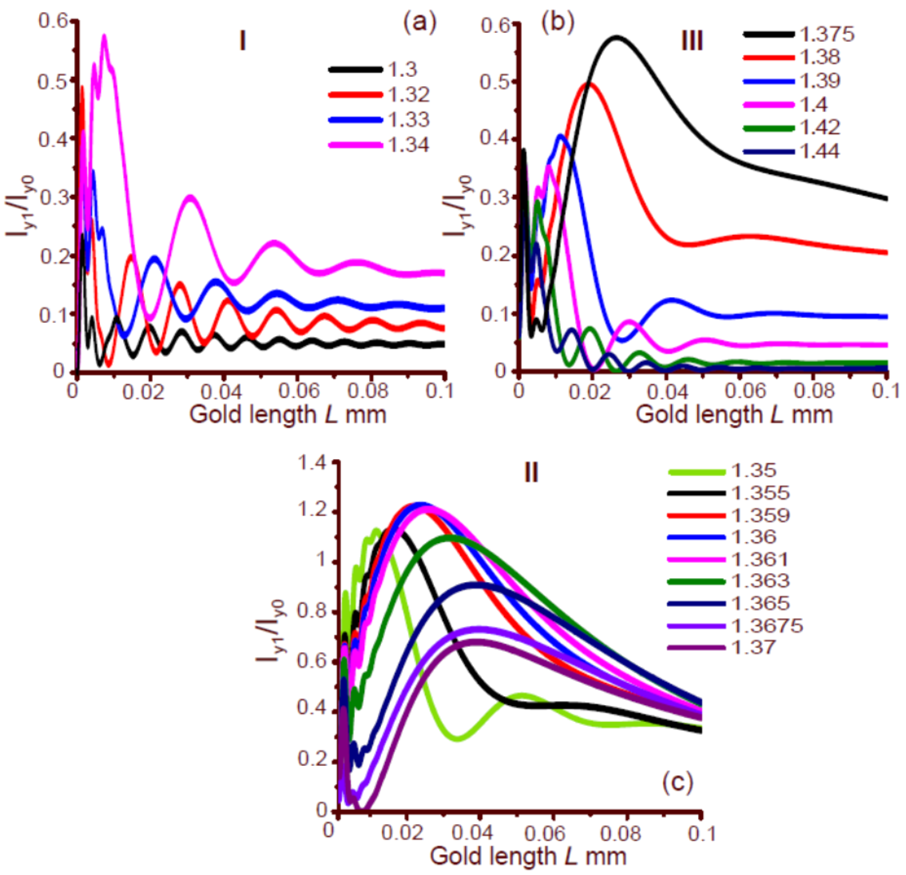

Figure 17: Calculated surface intensity profiles at $x = 0$ and along $L = 100\ \mu m$ [8].

Alina Karabchevsky, James S Wilkinson, and Michalis N Zervas. Transmittance and surface intensity in 3d composite plasmonic waveguides. Optics express, 23(11):14407-14423, 2015.

CALCULATED SURFACE INTENSITY

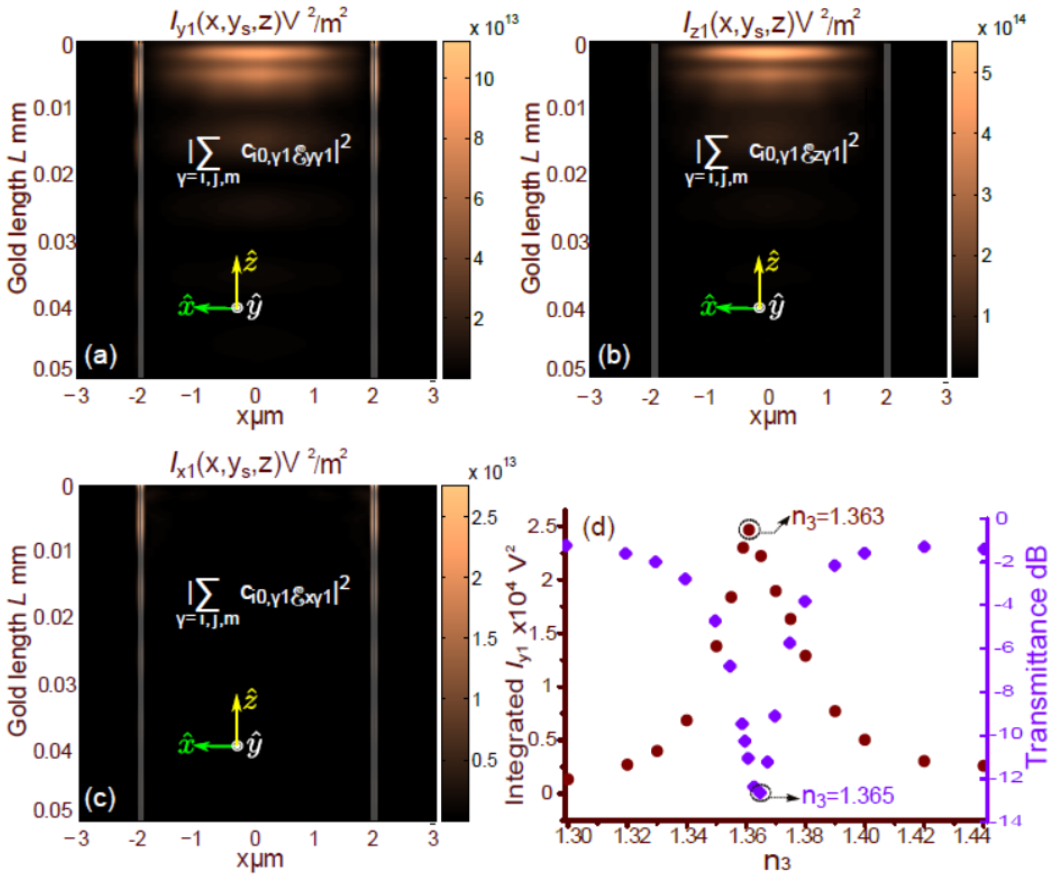

Figure 18: Mapped surface intensity [8].

Alina Karabchevsky, James S Wilkinson, and Michalis N Zervas. Transmittance and surface intensity in 3d composite plasmonic waveguides. Optics express, 23(11):14407-14423, 2015.

FIELD DISTRIBUTIONS - $z = L$

$$E_{xi2} = \sum_{\gamma=i,j,m} E_{x\gamma 1} \quad (51)$$

$$E_{yi2} = \sum_{\gamma=i,j,m} E_{y\gamma 1} \quad (52)$$

$$H_{xi2} = \sum_{\gamma=i,j,m} H_{x\gamma 1} \quad (53)$$

$$H_{yi2} = \sum_{\gamma=i,j,m} H_{y\gamma 1} \quad (54)$$

Multiplying Eq. (51) by H_{yi2} and Eq. (52) by H_{xi2} and subtracting between them leads to:

$$E_{x\gamma 1} H_{yi2} - E_{y\gamma 1} H_{xi2} = E_{xi2} H_{yi2} - E_{yi2} H_{xi2} \quad (55)$$

FIELD DISTRIBUTIONS - $z = L$

Multiplying Eq. (53) by E_{yi2} and Eq. (54) by E_{xi2} and subtracting between them leads to:

$$E_{yi2}H_{x\gamma 1} - E_{xi2}H_{y\gamma 1} = E_{yi2}H_{xi2} - E_{xi2}H_{yi2} \qquad (56)$$

Then, we are adding Eq. (55) and Eq. (56) and integrating over a whole range to obtain power carried in a mode i on the side 2 of the second step:

$$\iint_{-\infty}^{\infty}\left[\left(E_{\gamma 1} \times H_{i2}\right)_z + \left(E_{i2} \times H_{\gamma 1}\right)_z\right] dxdy =$$

$$= \iint_{-\infty}^{\infty}[(E_{i2} \times H_{i2})_z + (E_{i2} \times H_{i2})_z]dxdy \qquad (57)$$

$$= \iint_{-\infty}^{\infty} 2[(E_{i2} \times H_{i2})_z]dxdy$$

FIELD DISTRIBUTIONS - $z = L$

The field components as an amplitude and phase at the second step are:

$$E_\delta(x, y, L) = a_\delta \mathcal{E}_\delta(x, y) \exp(-j\beta_\delta L) \tag{58}$$

By substituting Eq. (51) and Eq. (54) into Eq. (57) we obtain:

$$a_{\gamma 1} a_{i2} \exp[-j(\beta_{\gamma 1} + \beta_{i2})L] \iint_{-\infty}^{\infty} \left[\left(\mathcal{E}_{\gamma 1} \times \mathcal{H}_{i2}\right)_z + \left(\mathcal{E}_{i2} \times \mathcal{H}_{\gamma 1}\right)_z \right] dxdy \tag{59}$$

which is equal to:

$$(a_{i2})^2 \exp[-j2\beta_{i2} L] \iint_{-\infty}^{\infty} [(\mathcal{E}_{i2} \times \mathcal{H}_{i2})_z + (\mathcal{E}_{i2} \times \mathcal{H}_{i2})_z] dxdy \tag{60}$$

FIELD DISTRIBUTIONS - $z = L$

by simplifying Eq. (59) = Eq (60), we obtain

$$a_{\gamma 1} \exp[-j\beta_{\gamma 1} L] \iint_{-\infty}^{\infty} \left[\left(\mathcal{E}_{\gamma 1} \times \mathcal{H}_{i2} \right)_z + \left(\mathcal{E}_{i2} \times \mathcal{H}_{\gamma 1} \right)_z \right] dxdy = a_{i2} \exp[-j\beta_{i2} L] \iint_{-\infty}^{\infty} [(\mathcal{E}_{i2} \times \mathcal{H}_{i2})_z + (\mathcal{E}_{i2} \times \mathcal{H}_{i2})_z] dxdy \qquad (61)$$

TRANSMITTANCE

$$T = \left|\frac{A_{i2}}{A_{i0}}\right|^2 = \left|\sum_{\gamma=i,j,m} c_{i0,\gamma 1} c_{\gamma 1,i2} \left(\frac{N_{i0}}{N_{i2}}\right)\right|^2$$

$$T = \left|\frac{A_{i2}}{A_{i0}}\right|^2 = \left|\sum_{\gamma=i,j,m} \frac{I_{i0,j1} + I_{j1,i0}}{2I_{j1,j1}} \frac{I_{\gamma 1,i2} + I_{i2,\gamma 1}}{2I_{i2,i2}} \exp(-j\beta_{\gamma 1} L)\right|^2 \qquad (62)$$

PREDICTION OF TRANSMITTANCE

Transmittance dB:

$$T = \left| \sum_{\gamma=i,j,k} \frac{\left(I_{i0,\gamma1} + I_{\gamma1,i0}\right)^2}{4I_{i0,i0}I_{\gamma1,\gamma1}} \exp\left(-j\beta_{\gamma1}L\right) \right|^2 \quad (77)$$

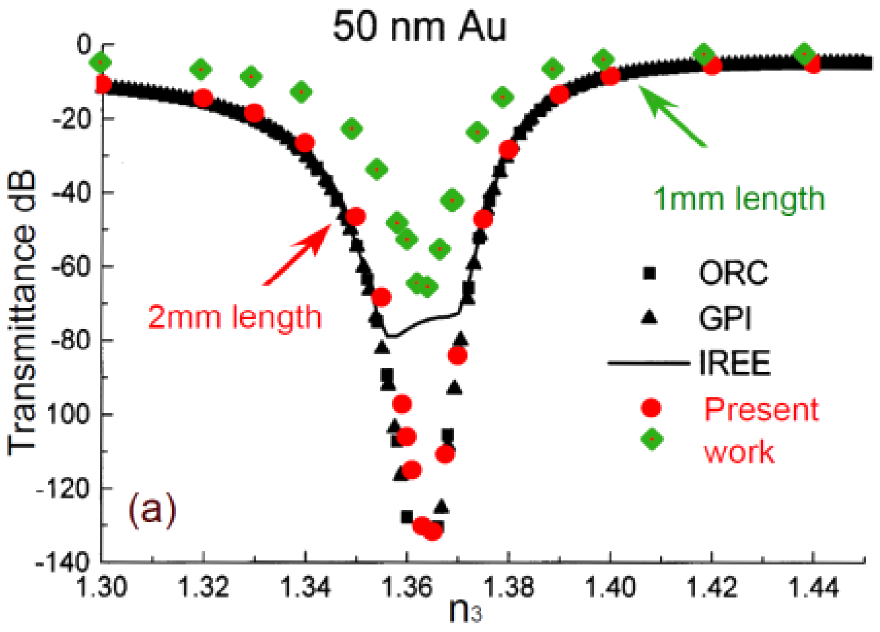

Figure 19: Calculated optical transmittance for $L = 2$ mm based on our model and of $L = 1$ mm [8].

Alina Karabchevsky, James S Wilkinson, and Michalis N Zervas. Transmittance and surface intensity in 3d composite plasmonic waveguides. Optics express, 23(11):14407-14423, 2015.

Relation of the fields at the second step to calculate the power are:

$$\mathcal{E}_{x\gamma 1} = \sum_{\gamma=i,j,m} c_{\gamma 1,i2}\mathcal{E}_{xi2} \tag{63}$$

$$\mathcal{E}_{y\gamma 1} = \sum_{\gamma=i,j,m} c_{\gamma 1,i2}\mathcal{E}_{yi2} \tag{64}$$

$$\mathcal{H}_{x\gamma 1} = \sum_{\gamma=i,j,m} c_{\gamma 1,i2}\mathcal{H}_{xi2} \tag{65}$$

$$\mathcal{H}_{y\gamma 1} = \sum_{\gamma=i,j,m} c_{\gamma 1,i2}\mathcal{H}_{yi2} \tag{66}$$

SUMMARY

- Theoretical study of planar waveguides with plasmonic overlayer.
- Coupling of hybrid real field distributions over a discontinuity in a waveguide horns.
- Mapping of surface intensity in 3D composite-plasmonic waveguides.
- Optical transmittance follows HDM modal attenuation loss.

ORTHOGONALITY OF COMPLEX MODES

- $\forall i \neq j \qquad I_{i,j} = 0$

$$E_{xi0} = \sum_{\gamma=i,j,m} E_{x\gamma1} \qquad (67)$$

$$E_{yi0} = \sum_{\gamma=i,j,m} E_{y\gamma1} \qquad (68)$$

$$H_{xi0} = \sum_{\gamma=i,j,m} H_{x\gamma1} \qquad (68)$$

$$H_{yi0} = \sum_{\gamma=i,j,m} H_{y\gamma1} \qquad (70)$$

MATCHING MODES EQUATIONS

$$\sum_{\gamma=i,j,m} A_{\gamma 1} = \sum_{\gamma=i,j,m} c_{i\gamma} A_{\gamma 0} \tag{71}$$

$$A_{\gamma 2} = \sum_{\gamma=i,j,m} c_{\gamma i} A_{\gamma 1} \tag{72}$$

$$c_{i\gamma} = \frac{I_{i0,\gamma 1} + I_{\gamma 1,i0}}{2I_{\gamma 1,\gamma 1}} \sqrt{\frac{\Re\{I_{\gamma 1,\gamma 1}\}}{\Re\{I_{i0,i0}\}}} \tag{73}$$

$$c_{\gamma i} = \frac{I_{\gamma 1,i2} + I_{i2,\gamma 1}}{2I_{i2,i2}} \sqrt{\frac{\Re\{I_{\gamma 1,\gamma 1}\}}{\Re\{I_{i0,i0}\}}} \tag{74}$$

Note: $I_{i2,i2} = I_{i0,i0} \quad \Rightarrow \quad I_{\delta,\delta} = \iint_{-\infty}^{\infty} (\bar{\mathcal{E}}_\delta \times \bar{\mathcal{H}}_\delta)_z \, dxdy$

NUMERICAL APPROACH

Figure 20: Cross-sections of the y-component of the electric field magnitude for the structure with a superstrate index of 1.4 in (a) a purely dielectric mode (DM) in a dielectric waveguide in the $z < 0$ and $z > L$ regions [8].

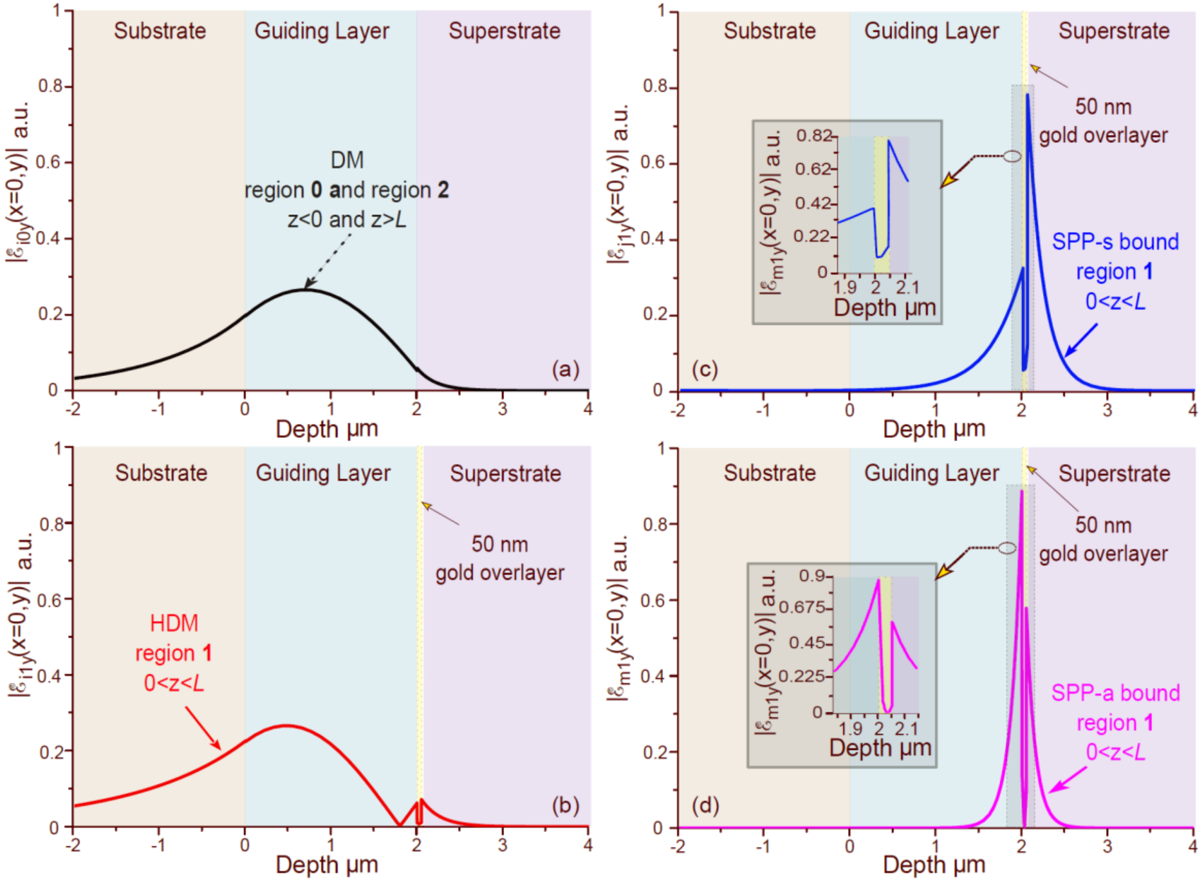

Alina Karabchevsky, James S Wilkinson, and Michalis N Zervas. Transmittance and surface intensity in 3d composite plasmonic waveguides. Optics express, 23(11):14407-14423, 2015.

MODES

Evolution of the dominant y-component of electric field magnitudes for quasi-transverse magnetic modes at resonance having superstrate index of 1.365, and far from it, at low superstrate index: 1.3 and high superstrate index 1.44 as labeled on the figure accordingly for DM, HDM, SPP-s and SPP-a guided modes [8].

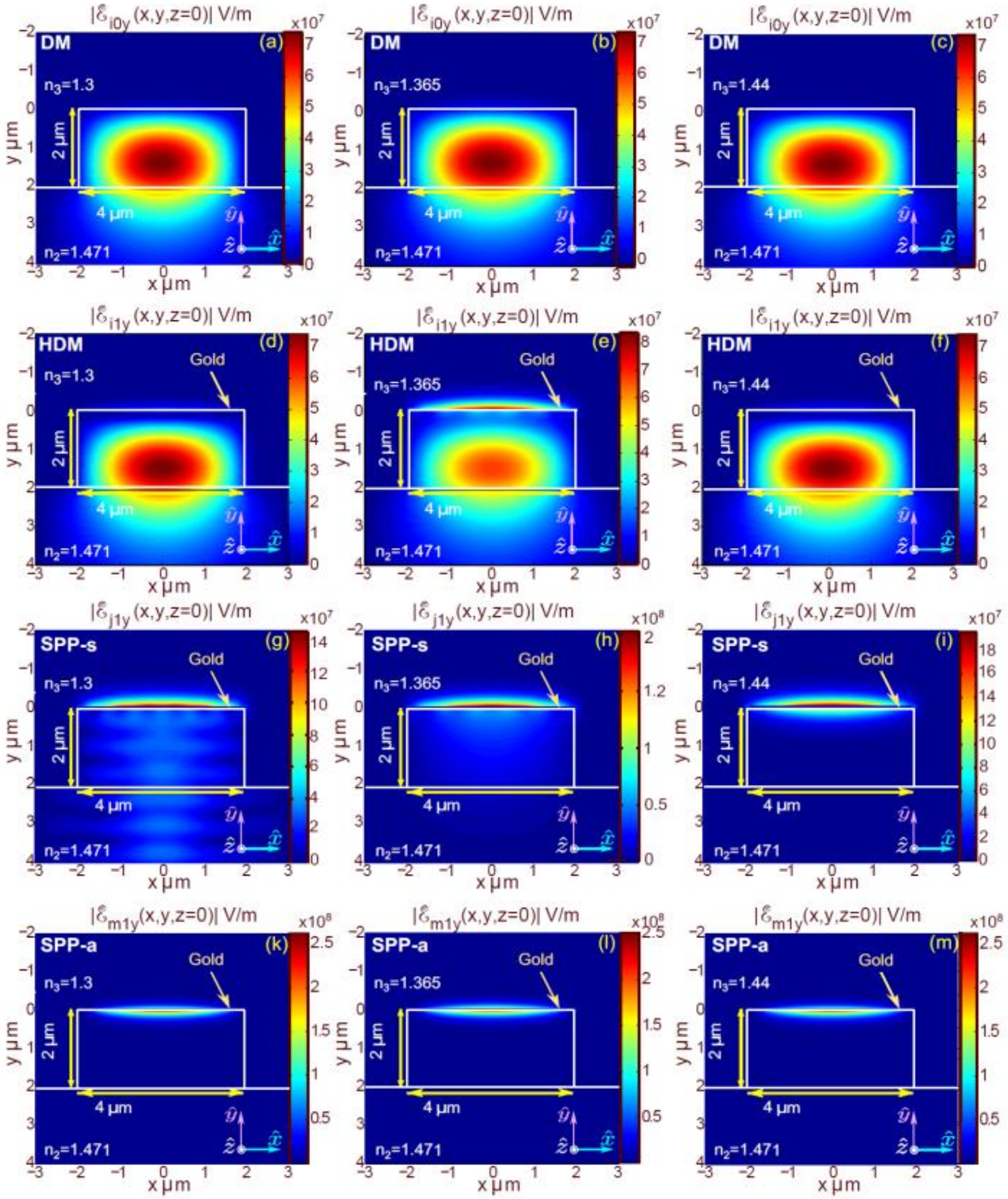

Alina Karabchevsky, James S Wilkinson, and Michalis N Zervas. Transmittance and surface intensity in 3d composite plasmonic waveguides. Optics express, 23(11):14407-14423, 2015.

ANALYSIS OF COMPLEX N_{eff}

Effective refractive index RIU:

$$N_{\mathrm{eff}} = \frac{\Re\{\beta\}\lambda}{2\pi} \tag{75}$$

Modal attenuation coefficient dB/cm:

$$\alpha = 0.2\log(e)\,\Im\{\beta\} \tag{76}$$

ANALYSIS OF COMPLEX N_{eff}

Figure 21: Variation of (a) effective refractive indices and (b) modal attenuation coefficients a in the gold-coated region $0 < z < L$ with n_3; (c) zoomed effective indices in the region enclosed in (a) [8].

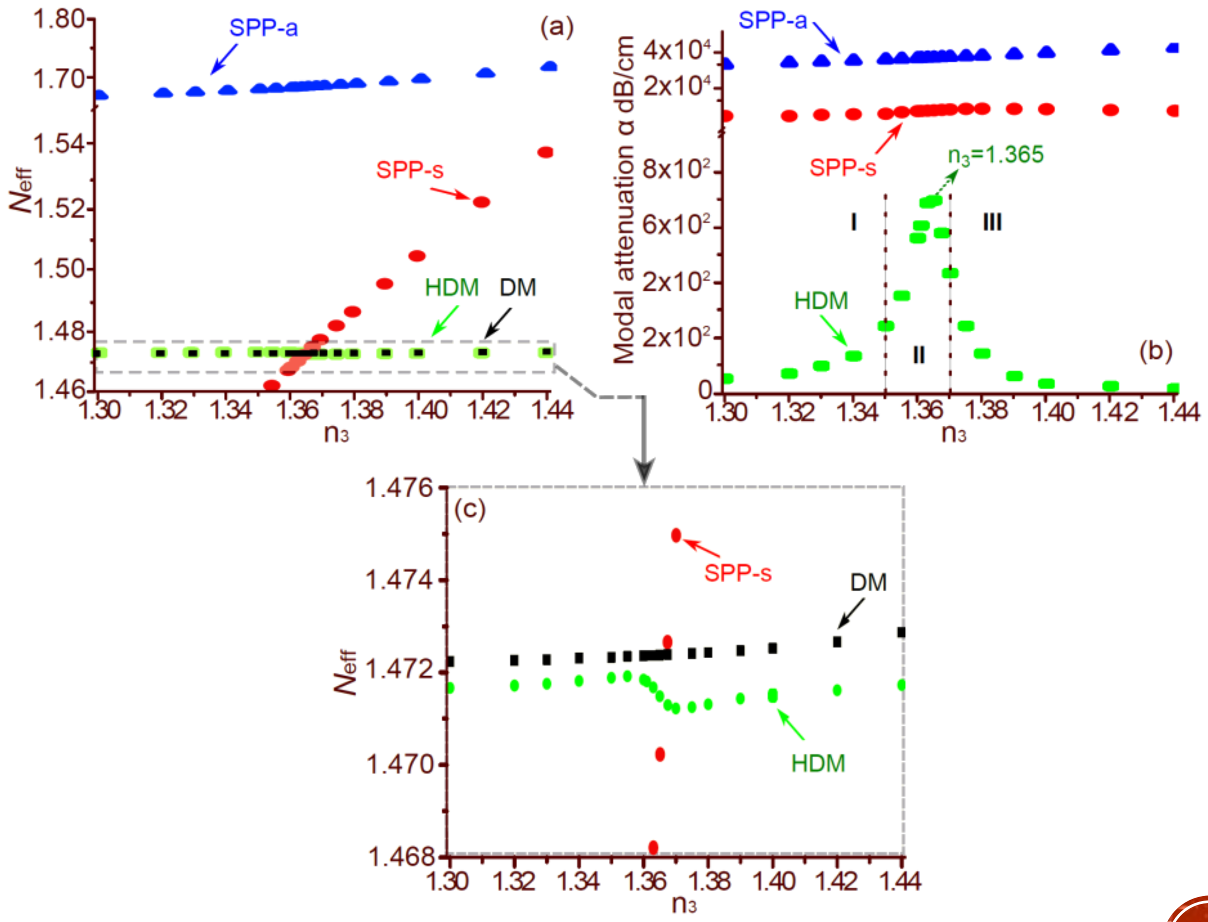

Alina Karabchevsky, James S Wilkinson, and Michalis N Zervas. Transmittance and surface intensity in 3d composite plasmonic waveguides. Optics express, 23(11):14407-14423, 2015.

SURFACE INTENSITY

Surface Intensity V^2/m^2:

$$I = \left| \sum_{\gamma=i,j,k} c_{i0,\gamma 1} \mathcal{E}_{\gamma 1} \right|^2 \tag{78}$$

Note: The superstrate indices, n_3 which yield the minimum in transmittance and the maximum in integrated surface intensity are labeled in (d).

SURFACE INTENSITY

Figure 22: Mapped surface intensity: (a) y component, (b) z component and (c) x component along 50 mm gold length for a superstrate index of 1.44 and (d) integrated surface intensity and transmittance for a $L = 200$ mm gold length vs. n_3 [8].

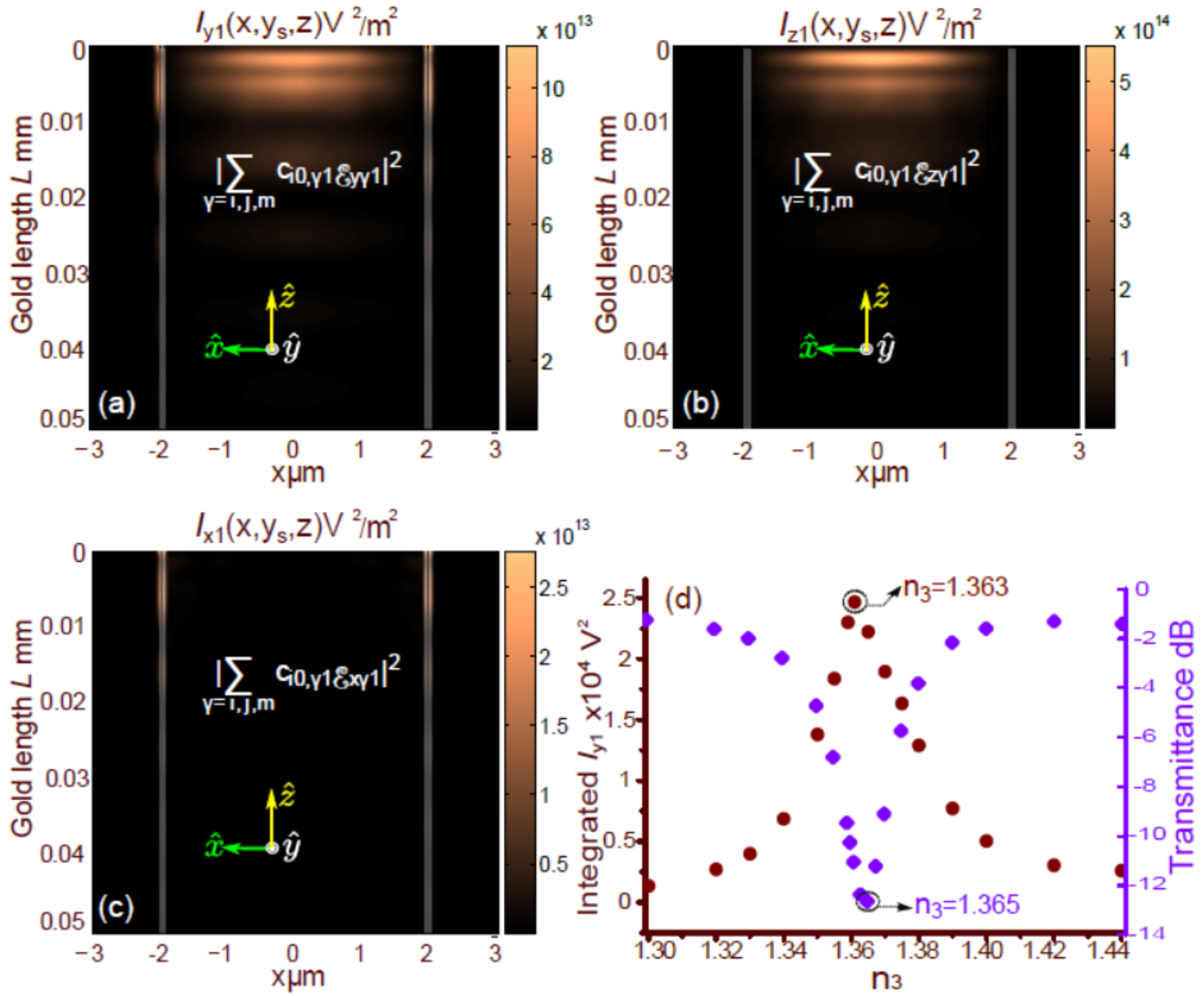

Alina Karabchevsky, James S Wilkinson, and Michalis N Zervas. Transmittance and surface intensity in 3d composite plasmonic waveguides. Optics express, 23(11):14407-14423, 2015.

CLOAKING WITH COMPOSITE PLASMONIC WAVEGUIDES

The interesting characteristics of composite plasmonic waveguides can be used to achieve novel devices. One of them is an invisibility cloak. Using transformation optics technique that is built upon two key observations:

- Maxwell's equations retain the same format under coordinate transformations in space, i.e. they are form-invariant under coordinate transformations.
- Maxwell's equations interpreted in different coordinate systems are equivalent to changing the medium parameters in the constitutive relationships.

TRANSFORMATION OPTICS

Consider a set of time-harmonic electric and magnetic fields $\tilde{\mathbf{E}}$ and $\tilde{\mathbf{H}}$ at an angular frequency ω in a cartesian (x, y, z) coordinate system. Adopting the $e^{j\omega t}$ time convention, the fields satisfy Maxwell's curl equations at any source-free point.

$$\nabla' \times \tilde{\mathbf{E}}' = -j\omega\mu'\tilde{\mathbf{H}}' \qquad (79)$$

$$\nabla' \times \tilde{\mathbf{H}}' = j\omega\varepsilon'\tilde{\mathbf{E}}' \qquad (80)$$

where the constitutive relationships

$$\tilde{\mathbf{B}} = \boldsymbol{\mu}\tilde{\mathbf{H}} \qquad \tilde{\mathbf{D}} = \boldsymbol{\varepsilon}\tilde{\mathbf{E}}$$

where $\tilde{\mathbf{D}}$ and $\tilde{\mathbf{B}}$ the electric and magnetic flux densities, respectively, $\boldsymbol{\varepsilon}$ is the electric permittivity tensor and $\boldsymbol{\mu}$ is the magnetic permeability tensor.

TRANSFORMATION OPTICS

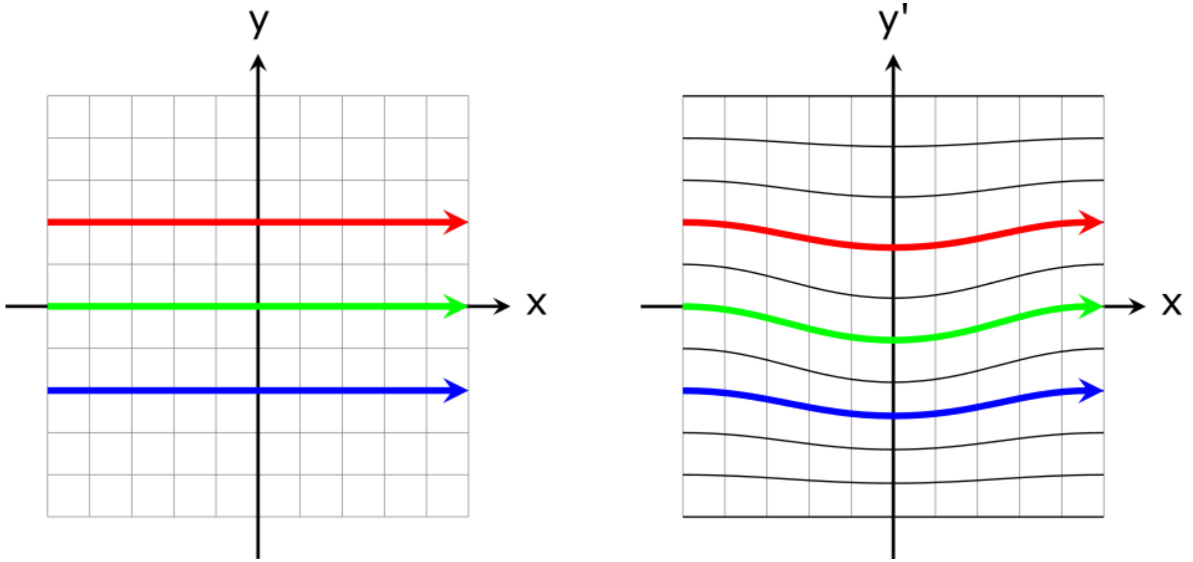

Since Maxwell's equations are form-invariant under coordinate transformations, the two curl equations in the transformed system may be written as:

$$\nabla' \times \tilde{\mathbf{E}}' = -j\omega\boldsymbol{\mu}'\tilde{\mathbf{H}}' \tag{81}$$

$$\nabla' \times \tilde{\mathbf{H}}' = j\omega\boldsymbol{\varepsilon}'\tilde{\mathbf{E}}' \tag{82}$$

TRANSFORMATION OPTICS

Let the coordinate transformation be described by the 3x3 Jacobian matrix A defined as:

$$\mathbf{A} = \begin{bmatrix} \partial x'/\partial x & \partial x'/\partial y & \partial x'/\partial z \\ \partial y'/\partial x & \partial y'/\partial y & \partial y'/\partial z \\ \partial z'/\partial x & \partial z'/\partial y & \partial z'/\partial z \end{bmatrix} \tag{83}$$

Both field and medium quantities in the (x', y', z') system are related to their respective counterparts in the (x, y, z) system. Specifically, the medium tensor parameters, μ_0' and ε_0', are related to μ_0 and ε_0 in the original space by the following expressions

$$\boldsymbol{\mu}' = \frac{\mathbf{A}\mu\mathbf{A}^T}{\det\{\mathbf{A}\}} \qquad \boldsymbol{\varepsilon}' = \frac{\mathbf{A}\varepsilon\mathbf{A}^T}{\det\{\mathbf{A}\}} \tag{84,85}$$

In addition, the fields in the transformed system are given in terms of the fields in the original system via

$$\tilde{\mathbf{E}}' = (\mathbf{A}^{-1})^T\tilde{\mathbf{E}} \qquad \tilde{\mathbf{H}}' = (\mathbf{A}^{-1})^T\tilde{\mathbf{H}} \tag{86}$$

THE COMPOSITE PLASMONIC WAVEGUIDE STRUCTURE

- Wavelength of $\lambda = 637$ nm illuminates the dielectric waveguide exciting the fundamental mode guided in region 0.
- Region 1 is characterized by the metasurface and Si nano-spacer placed on the waveguide with length L in the propagation direction exciting three hybrid plasmonic modes.
- Region 2 is identical to the region 0 in terms of the optical properties and functionality. A scattering object with optical index of 1.3 is placed on the metasurface.

THE COMPOSITE PLASMONIC WAVEGUIDE STRUCTURE

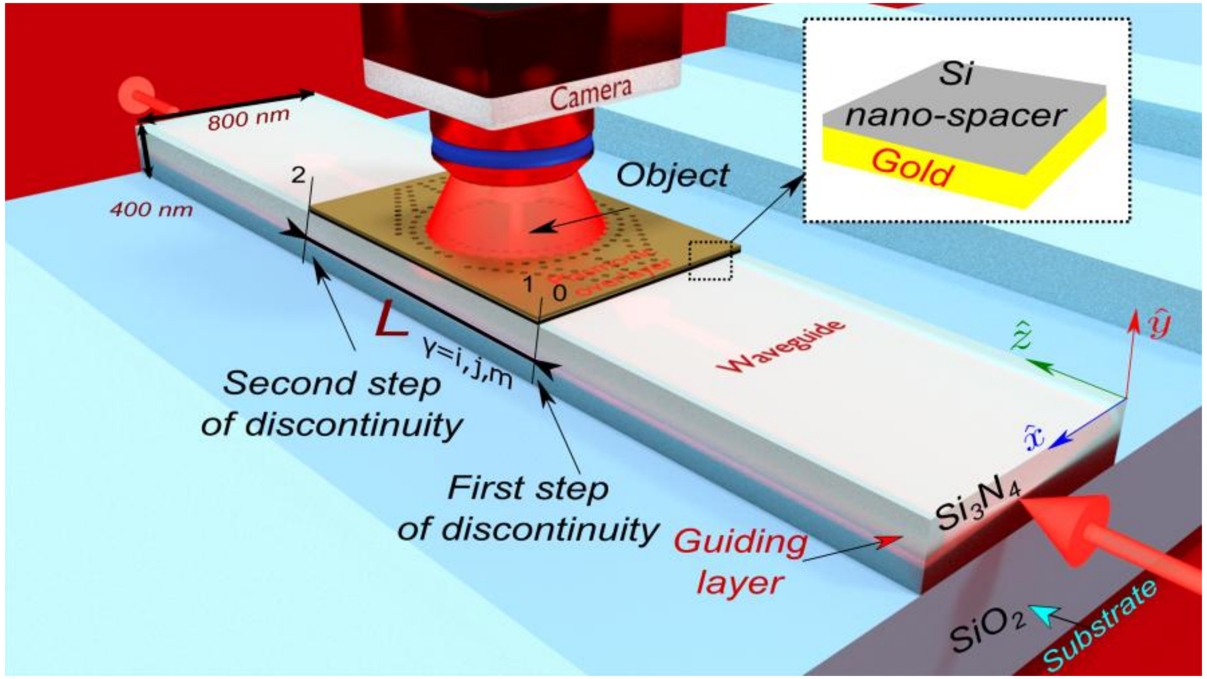

Figure 23: Illustration of the composite plasmonic waveguide structure and materials to study the invisibility cloaking scheme [9].

Yakov Galutin, Eran Falek, and Alina Karabchevsky. Invisibility cloaking scheme by evanescent fields distortion on composite plasmonic waveguides with si nano-spacer. Scientific reports, 7(1):12076, 2017.

COMPOSITE PLASMONIC WAVEGUIDE CLOAK DESIGN

If the mapping satisfies the Cauchy-Riemann conditions given by:

$$\partial x'/\partial x = \partial z'/\partial z \quad (87)$$

$$\partial x'/\partial z = -\partial z'/\partial z \quad (88)$$

the transformed material becomes inhomogeneous and isotropic. The resulting transformation is composed of a quasi-orthogonal grid with an effective index in each cell:

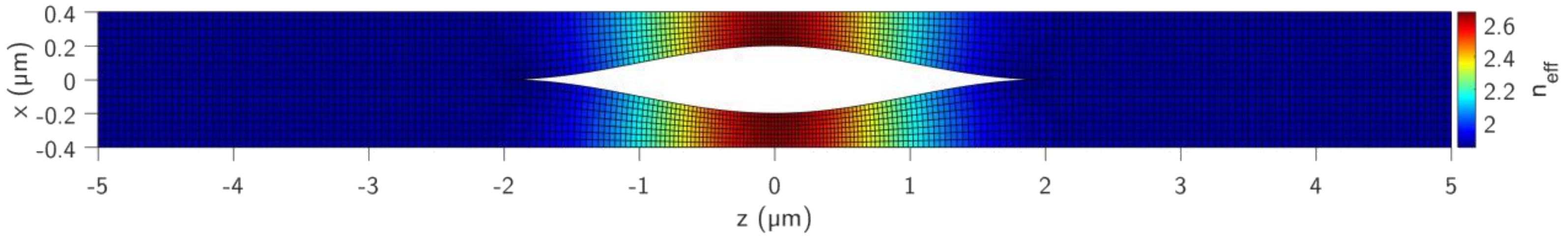

Figure 24: Transformed mesh using quasi-conformal transformation theme (black mesh) and calculated effective mode index, n_{eff} [9].

Yakov Galutin, Eran Falek, and Alina Karabchevsky. Invisibility cloaking scheme by evanescent fields distortion on composite plasmonic waveguides with si nano-spacer. Scientific reports, 7(1):12076, 2017.

CLOAKING RESULTS AND PERFORMANCE

The figure below shows calculated integrated total surface intensity to assess the effectiveness of evanescent invisibility cloak with a composite plasmonic waveguide.

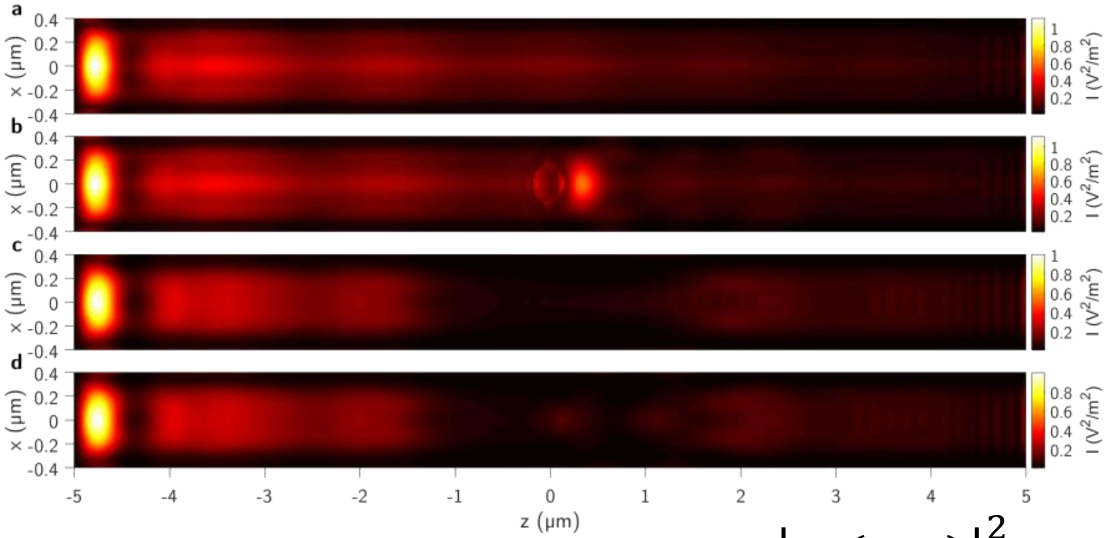

Figure 25: Calculated spatial surface intensities $|\varepsilon_y(x,y)|^2$ at $y = y_s$ in the composite plasmonic waveguide: (a) slab gold overlayer, (b) slab gold overlayer and an object index of 1.3, (c) transformed metasurface and (d) transformed metasurface and an object [9].

Yakov Galutin, Eran Falek, and Alina Karabchevsky. Invisibility cloaking scheme by evanescent fields distortion on composite plasmonic waveguides with si nano-spacer. Scientific reports, 7(1):12076, 2017.

BIBLIOGRAPHY

[1] Alina Karabchevsky, Olga Krasnykov, Mark Auslender, Benny Hadad, Adi Goldner, and Ibrahim Abdulhalim. Theoretical and experimental investigation of enhanced transmission through periodic metal nanoslits for sensing in water environment. Plasmonics, 4(4):281, 2009.

[2] Lukas Novotny and Bert Hecht. Principles of nano-optics. Cambridge university press, 2012.

[3] Hojjat Jodaylami, Maryam, Jean-François Masson, and Antonella Badia. "Surface plasmon resonance sensing." Nature Reviews Methods Primers 5.1 (2025): 47.

[4] Du, Bobo, et al. "SPR label-free biosensor with oxide-metal-oxide-coated D-typed optical fiber: a theoretical study." Plasmonics 14.2 (2019): 457-463.

[5] Bertolotti, Mario, Concita Sibilia, and Angela M. Guzman. Evanescent waves in optics: an introduction to plasmonics. Vol. 206. Springer, 2017.

[6] Ma, Hao, et al. "Surface-enhanced Raman spectroscopy: current understanding, challenges, and opportunities." ACS nano 18.22 (2024): 14000-14019.

[7] Neubrech, Frank, et al. "Surface-enhanced infrared spectroscopy using resonant nanoantennas." Chemical reviews 117.7 (2017): 5110-5145.

[8] Alina Karabchevsky, James S Wilkinson, and Michalis N Zervas. Transmittance and surface intensity in 3d composite plasmonic waveguides. Optics express, 23(11):14407-14423, 2015.

[9] Yakov Galutin, Eran Falek, and Alina Karabchevsky. Invisibility cloaking scheme by evanescent fields distortion on composite plasmonic waveguides with silicon nano-spacer. Scientific reports, 7(1):12076, 2017.